Kimberlite Diamond Deposits

B.A. Kjarsgaard

Geological Survey of Canada, 601 Booth Street, Ottawa, Ontario, K1A 0E8
Corresponding author's email: bruce.kjarsgarrd@nrcan.gc.ca

Abstract

Diamonds have formed over a significant period of the Earth's history, from ca. 3.57 Ga to 88 Ma, and probably to present day. Macrodiamonds are interpreted to crystallize from low-density fluids, or carbon- and water-rich melts at pressures >~4.0 GPa and temperatures <~1350°C. These P–T conditions are met within thick, old lithospheric mantle roots that have low paleogeothermal gradients, and these roots lie under ancient continental nuclei. Kimberlite-hosted diamond mines occur in these cratonic shield regions that are older than 2.5 Ga. Macrodiamonds are transported as xenocrysts from the mantle to the surface by kimberlite magmas. The initiation of kimberlite magmatism is at depth in the asthenospheric mantle (>150 km), although the initiation and generation of kimberlite magma is poorly understood. Kimberlites magmas generate a range of rocks that form a wide variety of landforms and intrusions, in many aspects similar to that generated by small-volume alkali basaltic volcanic systems. Kimberlite bodies typically form from multiple intrusive and/or extrusive events; these discrete events form distinct kimberlite phases. These individual kimberlite phases are characterized by differing textures, mineralogy and geochemistry, and diamond grade, size populations and morphology, and value.

Résumé

Des diamants se sont formés pendant une longue période de l'histoire de la Terre, de 3,57 Ga à 88 Ma environ, et se forment probablement encore de nos jours. Selon diverses interprétations, les macrodiamants se formeraient par cristallisation à partir de fluides de faible densité ou encore de bains magmatiques riches en carbone et en eau à des pressions supérieures à environ 4,0 GPa et à des températures inférieures à environ 1350 °C. Ces conditions de pression et de température sont atteintes à l'intérieur d'anciennes et épaisses racines de manteau lithosphérique caractérisées par de faibles paléogradients géothermiques, qui se situent sous d'anciens noyaux continentaux. Les mines de diamants dans des kimberlites gisent dans ces régions de boucliers cratoniques datant de plus de 2,5 Ga. Les macrodiamants sont transportés sous forme de xénocristaux depuis le manteau jusqu'à la surface par des magmas kimberlitiques. L'amorce du magmatisme kimberlitique se produit en profondeur dans le manteau asthénosphérique (>150 km), bien que le début de la formation et la production du magma kimberlitique soient des phénomènes encore mal compris. Les magmas kimberlitiques engendrent toute une gamme de roches donnant lieu à des formes de terrain et à des intrusions très variées, à de nombreux égards similaires à celles engendrées en de moindres volumes par les systèmes volcaniques de basalte alcalin. Les corps kimberlitiques se forment de manière caractéristique à partir de multiples événements intrusifs ou extrusifs; ces événements discrets forment des phases kimberlitiques distinctes, caractérisées par des différences de texture, de minéralogie et de géochimie ainsi que de la teneur en diamants et de caractéristiques de ceux-ci telles que la taille (populations granulométriques), la morphologie et la valeur des pierres.

Definition

Simplified Definition of Deposit Type

Primary deposits of diamonds occur in kimberlite as a sparsely dispersed xenocrystal mineral in pyroclastic, volcaniclastic, resedimented volcaniclastic and sub-volcanic (hypabyssal) rocks of mantle origin (kimberlite-hosted deposits). Secondary deposits formed by the weathering of primary deposits occur in unconsolidated and consolidated sediments (placers, paleoplacers, and volcanogenic sedimentary deposits).

Scientific Definition of Deposit Type

Kimberlite is formed from alkali-poor, H_2O- and CO_2-rich ultrabasic magma that has an enriched incompatible (Ba, Zr, Hf, Ta, Nb, REE) and compatible (Ni, Co, Cr) trace element signature. These magmas gave rise to rocks that form a wide variety of landforms and intrusions, similar to those exhibited by small-volume alkali basalt volcanic systems. Diamond xenocrysts are variably distributed throughout the host rocks at concentration levels of <0.01 to 2.0 ppm.

Deposit Subtypes

Lamproite and orangeite (also called Group II kimberlite) host primary magmatic diamond deposits. Placer and paleoplacer deposits can also be viewed as a subtype.

Distributions

Global Distribution of Kimberlite Diamond Deposits

Major producing or past-producing kimberlite-hosted diamond mines are known from southern Africa (South Africa, Botswana, Zimbabwe), south-central Africa (Tanzania, Democratic Republic of Congo, Angola), western Africa (Sierra Leone), Russia (Yakutia), China, Canada, and the United States (Fig. 1). These deposits are all found in Precambrian terranes and specifically in Archean continental blocks. The absence of kimberlite-hosted diamond mines in countries or continents with significant Archean crustal blocks such as Australia, India, and South America is notable, especially given the formerly significant paleoplacer and placer deposits in India and Brazil.

Kjarsgaard, B.A., 2007, Kimberlite diamond deposits, *in* Goodfellow, W.D., ed., Mineral Deposits of Canada: A Synthesis of Major Deposit Types, District Metallogeny, the Evolution of Geological Provinces, and Exploration Methods: Geological Association of Canada, Mineral Deposits Division, Special Publication No. 5, p. 245-272.

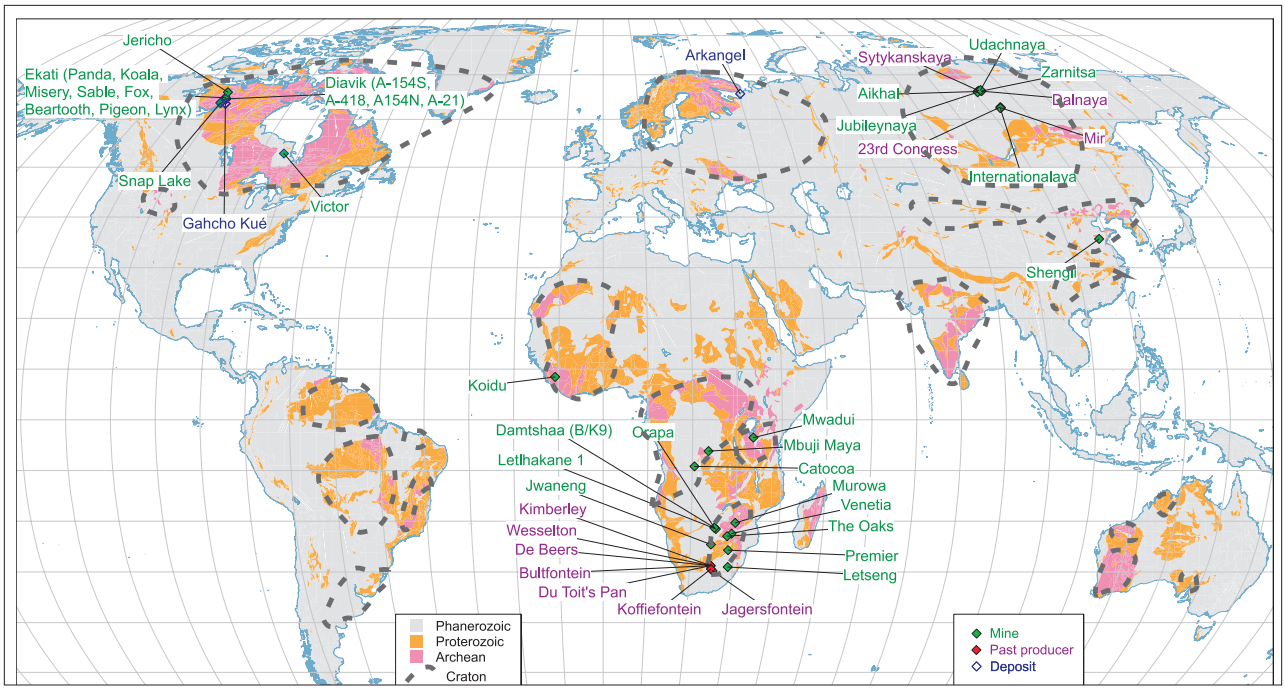

Figure 1. Global distribution of kimberlite-hosted diamond mines (active mines and past producers) and significant deposits. Also shown are the major Archean cratons.

Ages of Deposits

A significant observation is that there are specific time periods in the Earth's history when kimberlites with economically viable contents of diamonds erupted contemporaneously on different continents, for example, in Tanzania and Canada at ca. 52 to 56 Ma (Davis and Kjarsgaard, 1997) and in South Africa and Canada at ca. 535 to 542 Ma, whereas at other times kimberlite events are restricted to a specific region, e.g., Yakutia at ca. 360 Ma (Fig. 2; Heaman et al., 2003, 2004). The oldest kimberlite-hosted diamond mine is the Cullinan (or Premier) Mine in South Africa, which has been dated by radiometric methods at ~1200 Ma (Allsopp et al., 1989). The Venetia kimberlite in South Africa is of similar age to the Gahcho Kué #5034 pipe and the Snap Lake sill in the Slave Province, Northwest Territories (NWT), Canada (all ca. 542–535 Ma; Heaman et al., 2003). Kimberlites that host diamond mines in China are dated at ca. 475 to 462 Ma (Dobbs et al., 1994). The Yakutian kimberlites that host the economically important diamond mines have been dated by radiometric methods at ca. 376 to 344 Ma (Davis, 1977, 1978; Kinny et al., 1997), whereas the Jwaneng kimberlite in Botswana is ca. 235 Ma in age (Kinny et al., 1989). Numerous kimberlites hosting diamond mines in southern Africa, for example, Letseng, Lesotho; Jagersfontein, Koffiefontein, Du Toit's Pan, Bultfontein, De Beers, Kimberley and Wesselton in South Africa and Orapa in Botswana, are of similar age (ca. 95–84 Ma; Davis, 1977). Slightly younger in age are kimberlites that host the Mbuji Maya Mine in the Democratic Republic of Congo (71 Ma; Davis, 1977). The youngest kimberlites known to host diamond mines are found at the Ekati and Diavik Mines in the Slave province, NWT (56–53 Ma;

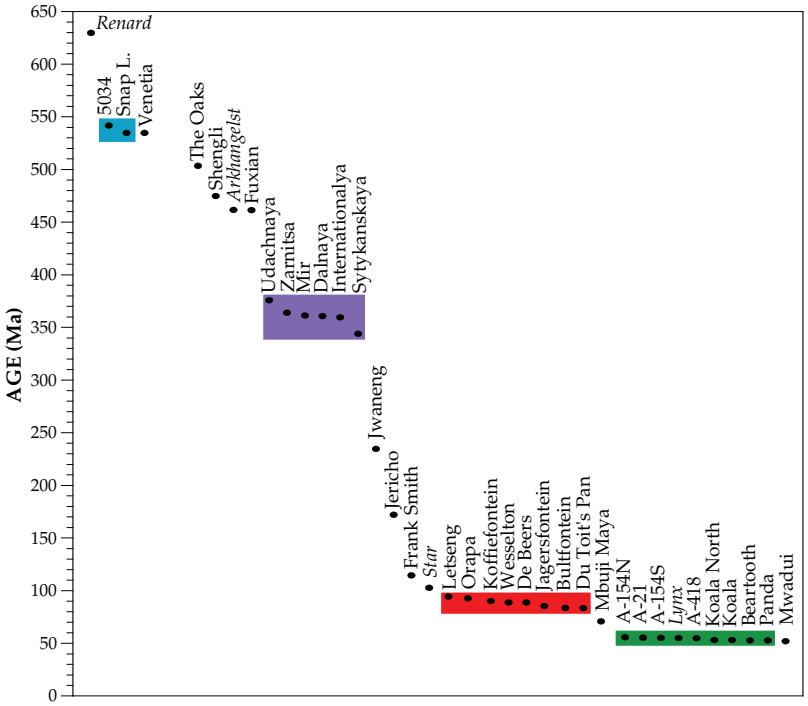

Figure 2. Emplacement ages of kimberlite-hosted diamond mines (past producers and active mines) and significant deposits. Data from Heaman et al. (2003, 2004).

Graham et al., 1999; Kjarsgaard et al., 2002; Creaser et al., 2004) and in Tanzania at the Mwadui Mine (52 Ma; Gobba, 1989).

Distribution and Age of Canadian Deposits

The kimberlites that comprise the Ekati, Diavik, Jericho, and Snap Lake mines all lie within the Contwoyto terrain of the Archean Slave province, as does the Gahcho Kué deposit (Fig. 3). The Jericho kimberlite in the north Slave is Jurassic in age (172 Ma). The central Slave kimberlites that host the Ekati (Panda, Beartooth, Koala) and Diavik (A-154N, A-154S, A-418, A-21) mines are Paleogene in age (56.0–53.0 Ma). The southeast Slave Snap Lake and Gahcho Kué (5034) kimberlites are of Cambrian age (523–535 Ma and 542 Ma, respectively), being significantly older (Fig. 2). The Victor diamond mine lies in the Archean Superior craton within the Sachigo sub-province (Fig. 3). Although the age of the Victor kimberlite has not been determined, most other kimberlites in the field have Jurassic emplacement ages in the range of 175 to 180 Ma (Heaman and Kjarsgaard, 2000). The Slave craton is estimated to contain ~US$27B (see Table 1) of diamonds in known economically viable deposits (Fig. 4a). The Superior province, in contrast, contains only one known mine (Victor), which is estimated to contain ~US$3.5B (see Table 1) of diamonds (Fig. 4a). The estimated value (see Table 1) of Canadian diamond deposits by age is:

- Middle Paleogene Ekati and Diavik mines at Lac de Gras contains ~US$19B of economically viable diamonds;
- Middle Jurassic Victor and Jericho deposits contain a ~US$4.1B of diamonds;
- Early Cambrian Snap Lake and Gahcho Kué deposits contains ~US$7.2B of diamonds (Fig. 4b).

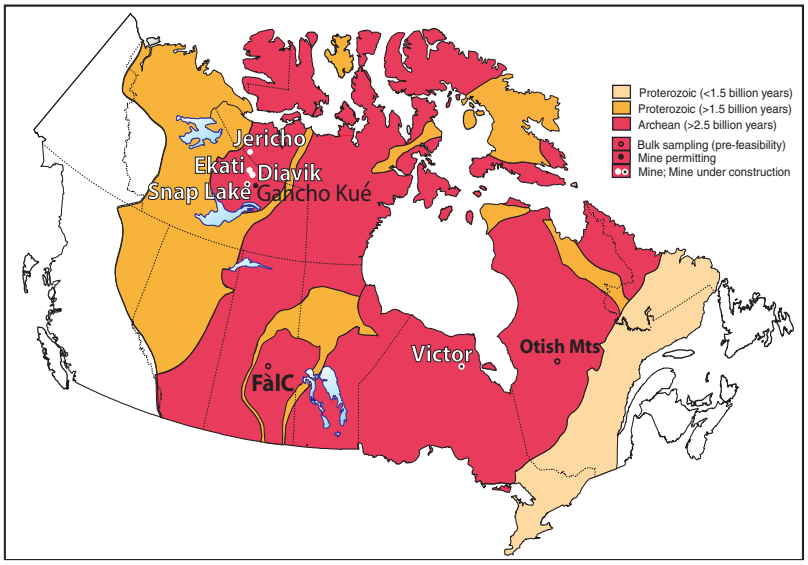

Figure 3. Geographic distribution of Canadian diamond mines, diamond deposits, and kimberlites that being bulk sampled as part of advanced exploration projects. Also shown are Proterozoic and Archean terranes (younger sedimentary cover sequences removed).

Pre-feasibility bulk sampling is currently being undertaken on the Cretaceous age ca. 103 Ma Star and Orion kimberlites in the Fort à la Corne area of central Saskatchewan

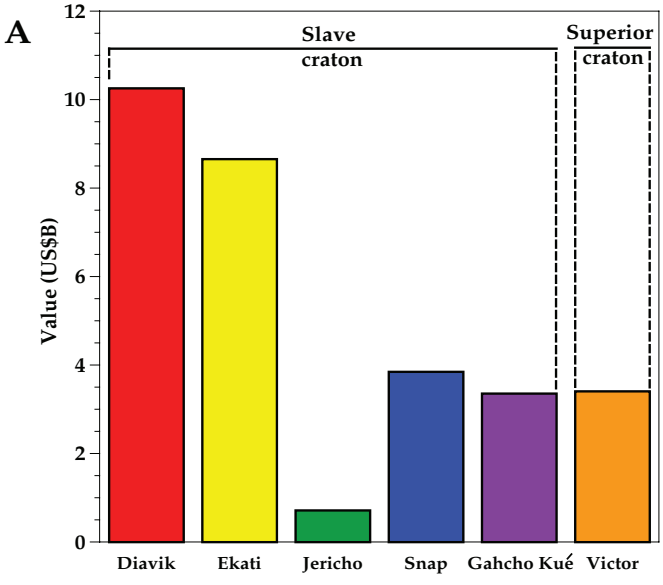

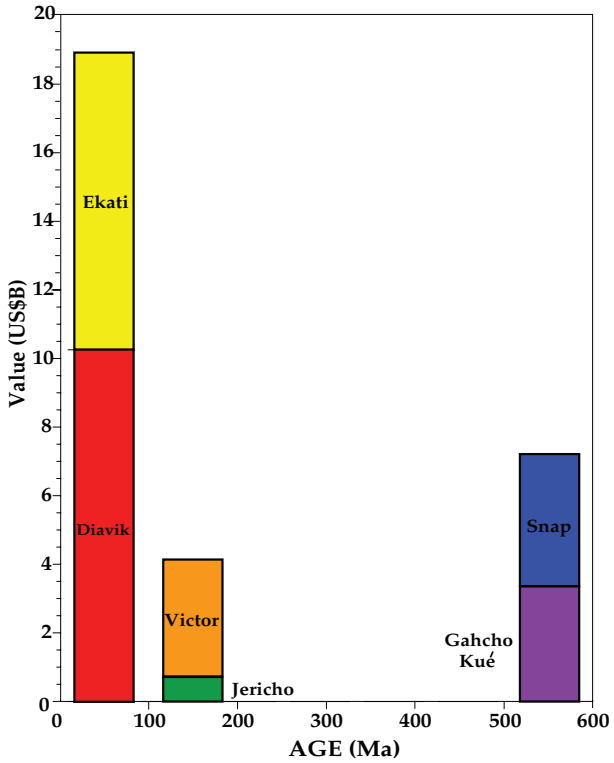

Figure 4. **(A)** In situ value of Canadian diamond mines and deposits subdivided by location with respect to Archean cratonic blocks. **(B)** In situ value of Canadian diamond mines and deposits subdivided by emplacement age.

Table 1. Canadian kimberlite mine diamond grade, stone value, ore value and tonnage data

PIPE	Grade (c/t) reserve	stone value US$/c reserve	Avg ore value US$/T reserve + resource	Area (ha) of pipe	Mt (tot) reserve	Grade ind/inf resource	MT ind/inf resource	Total tonnes (MT) reserve + resource	Avg grade (c/t) reserve + resource
A-154S	4.8	96	459	2.64	10.5	4.4	0.6	11.1	4.78
A-418	3.4	56	192	1.39	8.7	3.8	0.6	9.3	3.43
A-154N	3.1	82	248	1.23	10.6	2.5	1.6	12.2	3.02
A-21		28	76	1		2.7	4.8	4.8	2.70
Diavik total								**37.4**	
Panda	1.1	168	186	3.3	10.9			15.7	1.11
Panda u/g	1.4				1.4	1	3.4		
Koala	1	138	174	4.5	10	1	6.2	23.9	1.26
Koala u/g						1.2	13.9		
Koala North	0.5	143	72		0.1			1.7	0.50
Koala North u/g						0.5	1.6		
Misery	4.5	34	142	1.1	5.2	3.4	2.2	7.4	4.17
Sable	0.9	82	74	2.4	12.8	0.9	3.8	16.6	0.9
Fox	0.4	129	52	11	5.6	0.4	21.1	26.7	0.4
Beartooth	1.1	100	110	0.5	2	1.1	0.5	2.5	1.1
Pigeon	0.4	100	40	1	6.8	0.4	1.5	8.3	0.4
Lynx	0.8	108	86	0.6	1.4			1.4	0.8
Ekati total								**102.8**	
Jericho	1.2	85	102	3	2.6	0.63	4.5	7.1	0.84
Victor	0.23	458	105	5	32.4			32.4	0.23
Snap Lake	1.46	144	210	n/a	18.3			18.3	1.46
5034	1.6	82	134	1.95	8.7	1.7	4.9	13.6	1.64
Hearne	1.7	70	117	1.5	5.7	1.53	1.5	7.2	1.66
Tuzo		57	66	1.4		1.15	10.6	10.6	1.15
Gahcho Kue total								**31.4**	

Notes:
Diavik Mine grade and tonnage data as per end December 2004 from Aber Resources as reported by Aber Diamond Corporation (2005; see www.Sedar.com) with rough diamond value from Kjarsgaard et al. (2002) and The Northern Miner (2006b, v. 92 #7). Ekati Mine data as per end June 2003 for grade and tonnage from BHP-Billiton Annual Reports (J. Carlson, pers. comm, 2004); with rough diamond value from Kjarsgaard et al. (2002); Lynx data from The Northern Miner (2004, v. 90 #4). For the BHP Billiton data (other than Panda), the stone value and grade figures are exploration data and not run of mine and are probably low, and the stone values in Table 1 were determined over an approximate ten year period, during which time there was significant changes in the 'book' value for diamonds. Ekati Mine proven and probable ore reserves at June 2006 include: open cast, 31 Mt at 0.4 c/t; stockpile 1.2 Mt at 2.5 c/t; underground 11.8 MT at 0.9 c/t (from BHP-Billiton Annual Report 2007; note no stone values are given). Jericho Mine grade, tonnage and rough diamond value from Tahera Corporation (2003; see www.Sedar.com). Victor Mine and Snap Lake Mine grade, tonnage and rough diamond value from De Beers Canada factsheets (www.debeesrcanada.com) and The Northern Miner (2006a, v. 92 #2). Gahcho Kué deposit grade, tonnage and rough diamond value from De Beers Canada factsheets (www.debeesrcanada.com), The Northern Miner (2006a, v. 92 #2) and from Mountain Province Diamonds (2006; see www.Sedar.com). (2006a, v. 92, n. 2), and from Mountain Province Diamonds (2006; see www.Sedar.com).

and the Neoproterozoic age ca. 630 Ma Renard kimberlite in the northern Otish Mountains area of Quebec (Fig. 3).

Grade, Tonnage, and Value Statistics

Economic Characteristics of Global Diamond Deposits

Within a kimberlite diamond deposit, there is significant grade variation (typically greater than an order of magnitude) between individual intrusive phases and/or extrusive phases, and/or resedimented volcaniclastic phases (Fig. 5a). Furthermore, within an individual kimberlite phase in a diamond mine, there can also be significant grade variation (more than an order of magnitude; Fig. 5b). Hence, the compiled diamond grade data as shown in Figure 6a is based on interpreted average grades for mined out deposits, or 'head frame' grades for active mines. Also note that many diamond grades are inferred (e.g., Russian deposits) due to a lack of public domain data, or are based on data from exploration or feasibility studies, which may not be a true representation of

actual mine grades due to the small size of the preliminary samples. With these caveats in mind, diamond grade for economic diamond deposits ranges from ~0.02 to ~10 carats per tonne (carat/tonne), more than two orders of magnitude.

In contrast to the vast majority of commodities (e.g., metals), there is not a single value for diamond. The value of an individual rough diamond can be exceptionally variable (<US$1/carat to >US$1,000,000/carat), depending upon size, colour, and quality. For this reason, the average rough diamond value stated in US$/carat is a very important economic parameter. The known range for current and past producing mines is quite variable, ranging from ~US$15/carat to ~US$800/carat (Fig. 6b). Again, note that the caveats stated regarding diamond grade are also applicable to the average rough diamond value; for most active mines, the average rough diamond value is considered proprietary data. In this regard, some of the values shown in Figure 6b are probably low, due to use of exploration or feasibility sampling data. For example, the average value of rough diamonds from the Panda kimberlite from the feasibility study was US$130/carat, whereas the Panda run-of-mine rough diamond value increased ~30% to US$168/carat. This increase can be due to many factors, including lower stone breakage during mining as compared to reverse circulation drilling during exploration sampling, but perhaps more importantly mining typically recovers larger diamonds, which can strongly influence average rough diamond values (this is due to a statistical under sampling of the larger sieve classes of diamond in exploration or feasibility sampling, even when 3,000 to 10,000 carat parcels of diamond are recovered for evaluation purposes). An additional significant problem in comparing average rough diamond values is the fluctuation in book price over time (years to decades) due to supply and demand, and general economic conditions.

Kimberlite diamond deposits are quite variable in area (Fig. 6c) and geometry (dikes, sills, pipes, tephra cones). Due to a lack of public domain data, there is a paucity of ore tonnage reserve or resource data and even if the area of the kimberlite is known, it is difficult to calculate ore tonnage due to the variable geometry of these deposits. This is further complicated by the observation that not all of a kimberlite body may be economic with respect to diamond recovery. For example, the Letseng (Lesotho) kimberlite is 16 hectares (ha) in area, which would place it in the upper quartile for active or past producing kimberlite diamond mines. However, only the K6 phase at Letseng with an area of 4 ha was economic (Fig. 6c). Janse (1993) provided a novel approach to determining ore resource data worldwide by calculating tonnage to 120 m depth. Using this criterion, there are certainly very high tonnage (e.g., Mwadui, Orapa, Jwaneng, Premier) and very low tonnage (e.g., Koidu, The Oaks, Misery, A-154N) deposits.

Due to the wide range of diamond grades and rough diamond values for kimberlite diamond deposits, ore value expressed as US$/tonne (= grade [carat/tonne] × rough diamond value [US$/carat]) is one of the main parameters utilized in assessing the economic potential of a deposit (Figs. 6d, 7). Ore values range from ~US$13/tonne to ~US$1000/tonne.

Economic Characteristics of Canadian Deposits

The diamond grade for individual Canadian kimberlite pipes is highly variable (Kjarsgaard and Levinson, 2002). Five of the Lac de Gras kimberlite bodies (Ekati Mine Misery pipe and Diavik Mine A-154S, A-154N, A-418, A-21 pipes) have exceptional diamond grades (2.7–4.8 carats/tonne; Table 1) compared to active and past-producing diamond mines worldwide (Fig. 6a). These diamond grades, while remarkable for a kimberlite, are comparable to or low-

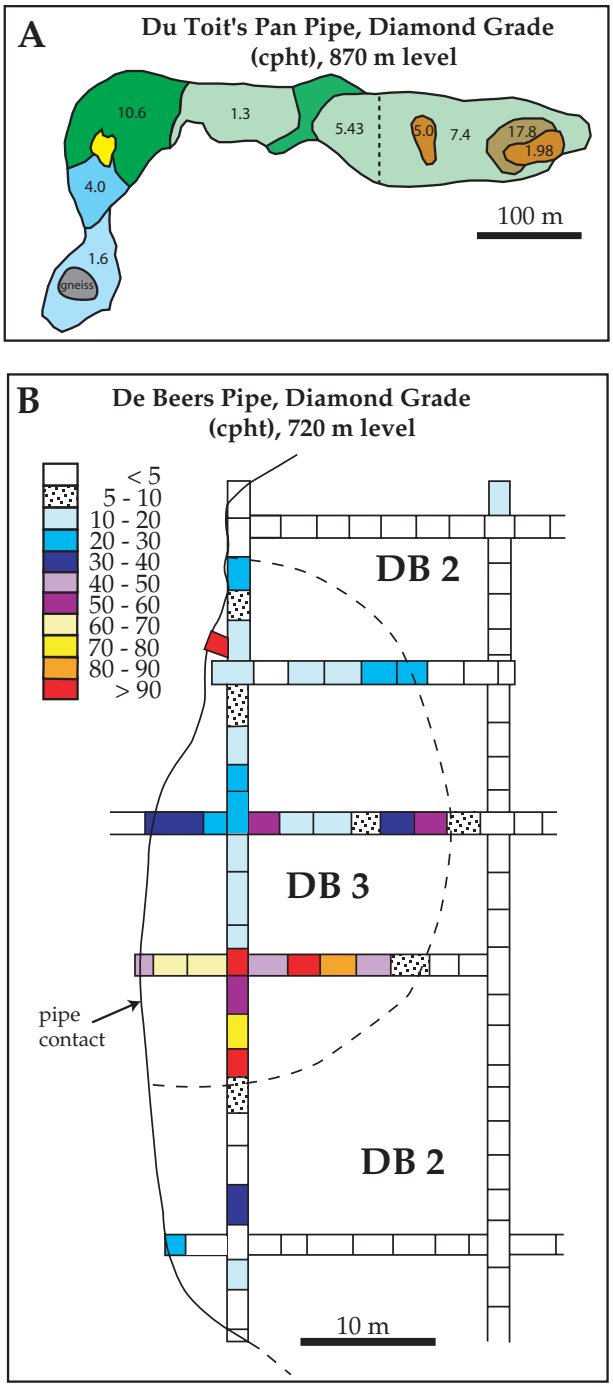

Figure 5. **(A)** Du Toit's Pan kimberlite, South Africa, 870 m level, illustrating the variation of diamond grade in cpht in relation to the different geological phases of kimberlite (after Clement, 1982). **(B)** De Beers kimberlite, South Africa, 720 m level, illustrating the variation of diamond grade in cpht within the DB2 and DB3 kimberlite intrusions (adapted from Clement, 1982). Note: cpht = carats per hundred tonnes.

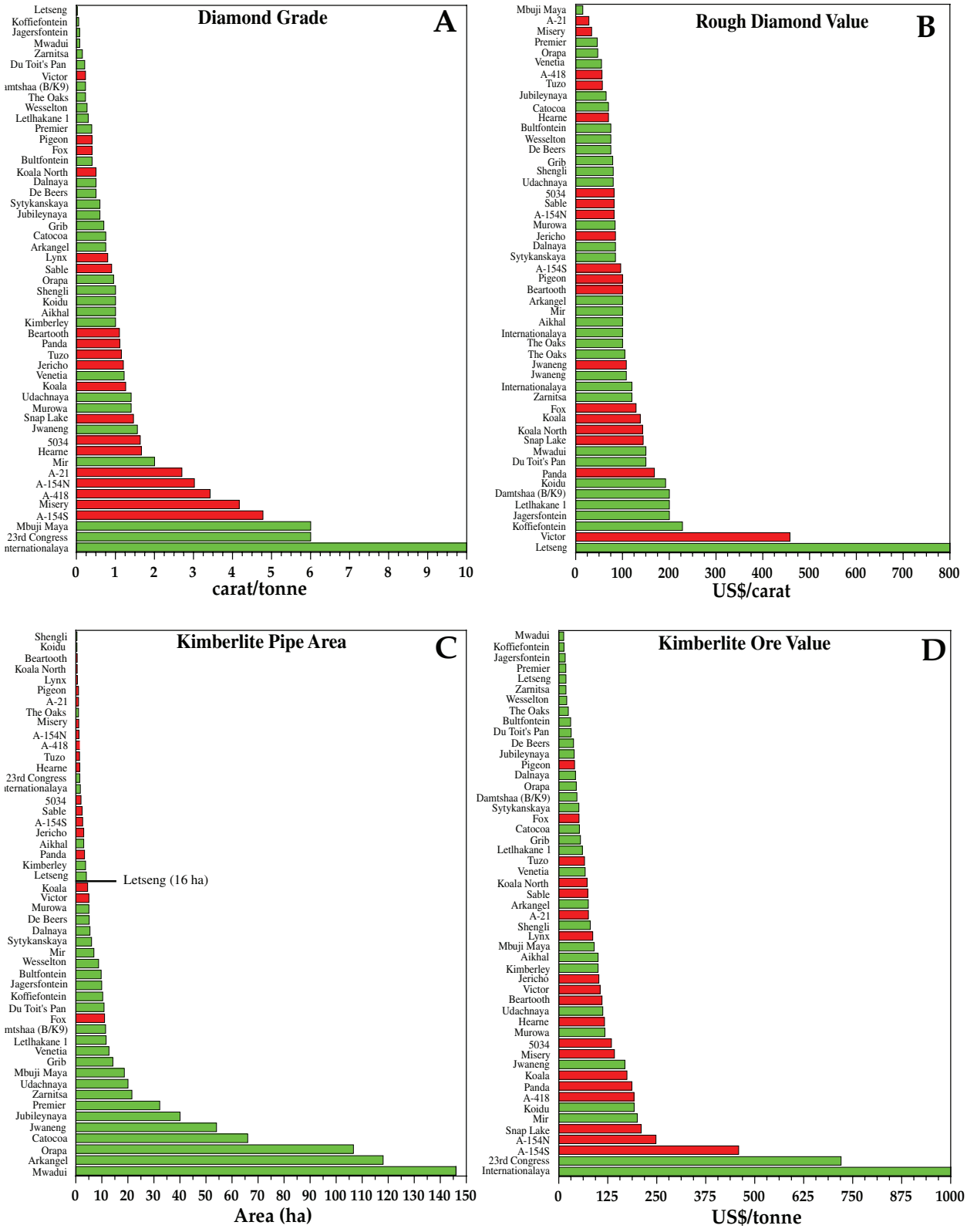

Figure 6. (A) Histogram illustrating the variation in diamond grade (in carats per tonne) for Canadian (red) and global (green) kimberlite diamond mines (active and past-producers). **(B)** Histogram illustrating the variation in rough diamond value (in US$ per carat) for Canadian (red) and global (green) kimberlite diamond mines (active and past-producers). **(C)** Histogram illustrating the range in hectares (ha) for Canadian (red) and worldwide (green) kimberlite diamond mines (active and past-producers). Note that the Letseng kimberlite total area is 16 ha, but the mineable part of the pipe was 4 ha. **(D)** Histogram illustrating the variation in ore value (in US$ per tonne) for Canadian (red) and global (green) kimberlite diamond mines (active and past-producers).

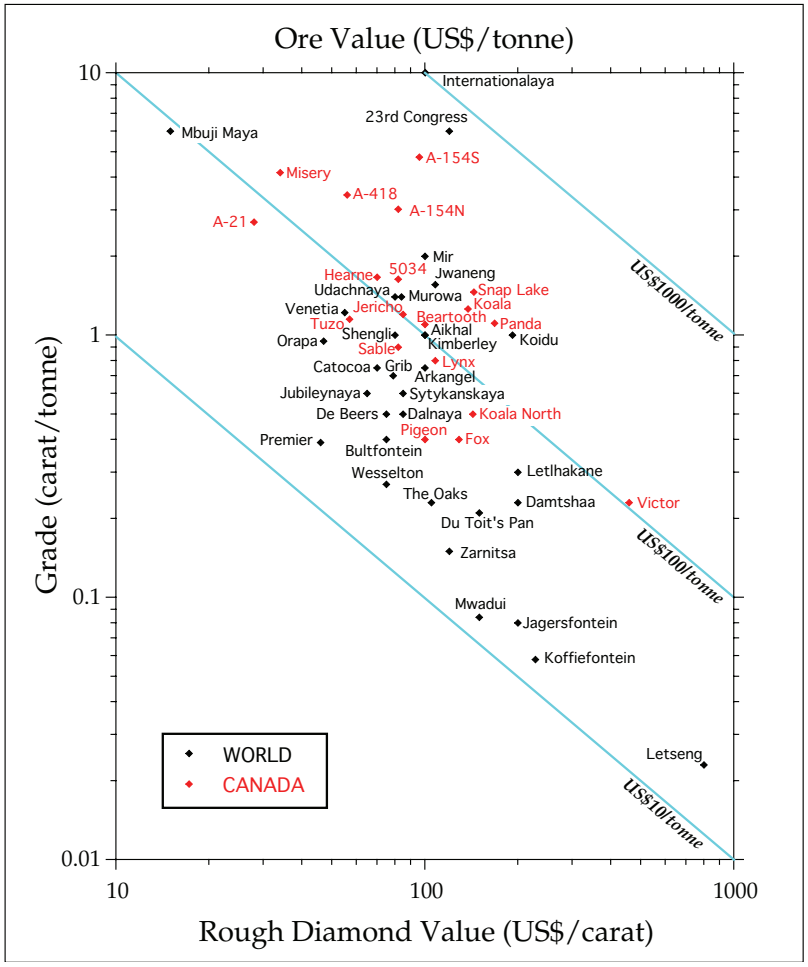

Figure 7. Log–log plot of diamond grade (carats per tonne) vs. rough diamond value (US$ per carat) for Canadian (red) and global (black) kimberlite diamond mines (active and past producers). This figure illustrates how kimberlites with quite disparate diamond grades and rough diamond values can have very similar ore values per tonne.

er than reported grades for Mbuji-Mayi (6 carats/tonne), 23rd Congress (6 carats/tonne), and Internationalaya (10 carats/tonne) kimberlites. The Hearne (1.67 carats/tonne), 5034 (1.64 carats/tonne), and Snap Lake (1.46 carats/tonne) kimberlites are high-grade diamond deposits (Table 1, Fig. 6a) and are in the upper echelon for grade as compared to active and past-producing diamond mines worldwide, for example, Mir, Jwaneng, and Murowa. Seven Canadian kimberlites, including the Koala, Jericho, Tuzo, Panda, Beartooth, Sable, and Lynx kimberlites, have average diamond grades ranging from 1.2 to 0.8 carats/tonne as compared to active and past-producing diamond mines worldwide (Table 1, Fig. 6a). The Koala North, Pigeon, Fox, and Victor kimberlites are of lower diamond grade (0.5–0.23 carats/tonne; Table 1, Fig. 6a).

There is a large variation in the average rough diamond value (quality) for individual Canadian kimberlite pipes. The Victor kimberlite has exceptionally valuable rough diamonds, averaging US$458/carat, and is only exceeded in value by diamonds from the Letseng (Lesotho) kimberlite (US$800/carat). The Panda (US$168/carat), Snap Lake (US$144/carat), Koala North (US$143/carat), Koala (US$138/carat), and Fox (US$129/carat) kimberlites all contain high-value diamonds (Table 1, Fig. 6b) and are in the upper echelon for rough diamond value as compared to active or past-producing diamond mines worldwide, for example, Koffiefontein, Letlhakane, and Damstshaa. The Lynx, Beartooth, Pigeon, A-154S, Jericho, A-154N, Sable, and 5034 kimberlites have rough diamond values ranging from US$82/carat to US$108/carat (Table 1, Fig. 6b); these diamond values are all higher than the world average rough diamond value of ~US$68/carat (based on 2004 world production data from Janse, 2005). Canadian kimberlites with low diamond values, for example, Misery (US$34/carat) or A-21 (US$28/carat), have average stone values approximately twice that of Mbuji Maya (US$15/carat).

The average to very small area (< 5 ha) of the known viable economic Canadian kimberlite pipes (with the exception of the 11 ha Fox pipe) is evident from Figure 6c. To date, economically viable Canadian kimberlites are significantly smaller than active diamond mines worldwide, the majority of which are >11 ha in area, although this observation would change if any of the very large (to 200 ha) Fort à la Corne kimberlites are mined.

There is a large variation in the value of ore for individual Canadian kimberlite pipes. The Diavik Mine A-154S kimberlite has an exceptional ore value of US$459/tonne, exceeded worldwide only by the Internationalaya (US$1000/tonne) and 23rd Congress (US$720/tonne) kimberlites in Russia (Figs. 6d, 7). The A-154N, Snap Lake, A-418, Panda, and Koala kimberlites all have very high ore values (US$248/tonne to US$170/tonne; Table 1, Figs. 6d, 7) that are in the upper echelon for ore values as compared to active or past-producing diamond mines worldwide, for example, Mir, Koidu, and Jwaneng. An additional six Canadian kimberlites (Misery, 5034, Hearne, Beartooth, Victor, and Jericho) have high ore values (>US$100/tonne; Table 1, Figs. 6d, 7). Ore values for the Lynx, A-21, Sable, Koala North, Tuzo, Fox, and Pigeon kimberlites are lower at 86, 76, 74, 72, 66, 52, and 40 US$/tonne, respectively (Table 1, Figs. 6d, 7).

In summary, economic Canadian kimberlite pipes tend to be small in area (low tonnage) bodies, that have variable (typically moderate to very high) diamond grades coupled with quite variable (low to very high) rough diamond values. These kimberlites have moderate to very high ore values, with the majority having ore values >US$100/tonne (Figs. 6d, 7). The development of the Ekati (eight orebodies) and Diavik (four orebodies) mines in the Lac de Gras area, Northwest Territories (NWT), required multiple economic pipes within a defined area so as to provide sufficient tonnage for a 15 to 20 year mine life. This is also true of the proposed Gahcho Kué diamond mine (three orebodies) in the NWT. An additional important factor regarding the economics of potential diamond mines in Canada is the operat-

ing cost. This will vary with mining method, for example, open pit versus underground mining, and the availability of infrastructure, for example, remote areas of Canada's north (the NWT, Nunavut, northern Ontario, and Québec) versus non-remote (southern to central Ontario, Quebec, and the prairie provinces). These two factors combined can result in potential operating costs varying by an order of magnitude (~US$10/tonne to US$100/tonne).

Contribution of Canadian Rough Diamonds to the World Supply

In 2004, combined diamond production from the Ekati and Diavik mines totaled 12.6 million carats, valued at US$2.1 billion (Perron, 2004). Canadian diamond production in 2004 comprised ~8% of world production by weight, but more importantly, ~16% of world production by value (2004 world production data from Janse, 2005). Compared to other producing countries, Canada ranked third by value (after Botswana and Russia) and sixth by number of carats produced. In 2004, Canadian diamonds from the combined output of the Ekati and Diavik Mines averaged ~US$135/carat, double the world average carat value of ~US$68/carat (based on 2004 world production data from Janse, 2005).

In 2006, Tahera's recently commissioned Jericho diamond mine started production. This mine will contribute an additional ~0.4 million carats/year for the next eight years, once full production is reached in 2007. By the end of this decade, additional rough diamond supplies will be coming on stream from the De Beers Victor (0.6 million carats/year) and Snap Lake (1.5 million carats/year) diamond mines. De Beers is also in the process of permitting the Gahcho Kué diamond deposit, which would have an output of 3 million carats/year. In summary, by 2010 Canada will likely be producing in excess of 15 million carats of rough diamond per year.

Geological Attributes

Continental Scale

Geotectonic Environment

Kimberlite diamond deposits are found within ancient Precambrian terrains older than 1.5 Ga (Clifford, 1966; "Clifford's Rule"). Diamond (i.e., macrodiamonds as opposed to microdiamonds) requires specific pressure and temperature conditions to form and remain stable with respect to graphite. These P–T conditions (typically > 4.0 GPa and < 1350ºC) are met within thick, old lithospheric mantle roots with low paleogeothermal gradients that typically lie under ancient continental nuclei. Modern geochronology of Precambrian terrains has led to better temporal understanding of the formation of continental nuclei, which Janse (1984; "Janse's Rule") utilized to suggest kimberlite diamond deposits are in fact found within Archean continental blocks (Fig. 1).

Recent radiometric age determinations of mineral inclusions in macrodiamonds (see summaries in Pearson and Shirey, 2002; Gurney et al., 2005) indicate that the oldest diamonds (peridotite paragenesis, or P-type) formed within the Earth's mantle no earlier than 3.57 Ga. A corollary is that Eoarchean (>3.6 Ga) continental blocks (with Eoarchean mantle roots) are not good targets for diamond exploration, perhaps because the early Earth was too hot and/or the lithospheric mantle to thin for diamonds to form and/or remain stable within the mantle. Pearson and Shirey (2002) and Gurney et al. (2005) have noted that the youngest known diamond formation event is Cretaceous, and that many kimberlite diamond mines contain diamonds that formed at different times in the Earth's history, concluding that diamond formation is episodic. It should be noted that a very limited amount of data is available regarding diamond formation age, and it is highly likely that diamonds are currently forming in the mantle.

The known ages of diamond formation can be utilized to suggest that the most promising exploration targets will be Paleoarchean continental blocks followed by Mesoarchean and Neoarchean blocks, and then Paleoproterozoic continental blocks. The rationale is simply that Paleoarchean mantle roots have the possibility of experiencing the highest number of potential diamond forming events, followed by Mesoarchean mantle roots, Neoarchean mantle roots, and Paleoproterozoic mantle roots. This idea is only valid if the crust and the mantle are coupled, for example, Mesoarchean continental crust overlies Mesoarchean mantle lithospheric roots. In general, this is usually true although there are certainly exceptions (Pearson, 1999a,b). For example, at the Fort à la Corne kimberlite field in central Saskatchewan, Paleoproterozoic rocks of the Trans Hudson Orogen overlie Archean rocks of the Sask craton (Ashton et al., 2005). The lamproite-hosted Argyle diamond mine (Australia), emplaced into the Paleoproterozoic Halls Creek mobile belt in a seemingly "off craton" environment, is however, underlain by Archean age lithospheric mantle (Luguet et al., 2005).

Eclogite paragenesis diamonds (E-type), on the basis of radiometric age determinations on inclusions in diamond, formed from 2.9 to 1.0 Ga. Detailed major-, trace-element and isotopic studies on kimberlite-derived eclogite xenoliths (Jacob, 2004; Jacob et al., 2005) and stable isotopic data on eclogite paragenesis diamonds (e.g., Gurney et al., 2005) indicate a subduction origin. Hence, a second important criteria at continental scale is Archean crust with Archean mantle roots that have experienced (distal) Archean to Mesoproterozoic subduction processes.

It has been previously suggested that certain geological events destroyed diamond-bearing lithospheric mantle roots. Helmstaedt (2003) argued that plume heads associated with basic igneous events, magmatic underplating associated with voluminous basic igneous events, and large scale plate collisions are all processes that destroy lithospheric mantle roots and their contained diamonds. The study of Read et al. (2004) in the Minais Gerais State, Brazil definitively illustrates that over a short time period (<10 m.y.) approximately 75 km of diamond-bearing lithospheric mantle root was removed or destroyed, related to the eruption of voluminous alkaline basic kamafugitic magma. However, the Premier diamond mine lies within the Bushveld complex (and has sampled mantle xenoliths that represent underplated basic magma; Hoal, 2003), which would suggest that voluminous basic magmatism and underplating is not always diamond unfriendly. Furthermore, the observation that the Venetia and The Oaks diamond mines

lie in the Limpopo collision belt between the Kaapvaal and Zimbabwe cratons does not support the notion that large-scale plate collisions destroys lithospheric mantle roots and their contained diamonds.

Distribution and Structural Control of Kimberlite Fields within Cratons

The distribution of kimberlite fields within a prospective (cratonic) region of old crust/mantle typically follows a broad linear pattern. This is observed, for example, in Yakutia (Bardet, 1965; Kaminsky et al., 1995). In the Slave craton the kimberlite fields follow a northwest trend from Kennedy Lake through Lac de Gras to northern Napatulik Lake (Fig. 8). Similarly, kimberlite fields in the Superior craton of Ontario follow a broad northwest trend (Fig. 8). Kaminsky et al. (1995) suggest these broad linear zones are areas of long-lived deep-seated major faults. This hypothesis may be applicable to kimberlite fields in Ontario (Fig. 8) with respect to the Lake Timiskaming structural zone (often incorrectly referred to as a rift). In contrast, in the Slave craton the kimberlite fields may be located above or proximal to the leading edge of the Mesoarchean central Slave basement complex (as defined by Bleeker et al., 1999).

The idea of pronounced structural control on the distribution of kimberlite fields, clusters, and pipes is not new (see Marsh, 1973; Nixon 1973; Haggerty, 1982; Mitchell, 1986, Coopersmith, 1993; White et al., 1995; and Jelsma et al., 2004). Structures such as deep fractures or shear zones (cryptic lineaments) are often apparent on aeromagnetic maps and digital elevation models according to Kaminsky et al. (1995) and Jelsma et al. (2004), with most kimberlite fields occurring at the intersections of two or more of these major structures. Jelsma et al. (2004) suggest these fractures or zones extend into the mantle and are re-activated over time. In Ontario, the Timiskaming, Kirkland Lake, and Attawapiskat fields are all at the intersection of major easterly trending structures with the northwest-trending Lake Timiskaming structural zone. Within a kimberlite field, some kimberlite clusters of small aerial extent contain multiple kimberlite-hosted diamond mines. This is certainly true for the five Kimberley area mines within the Kimberley cluster of South Africa and the twelve kimberlites (in two distinct clusters)

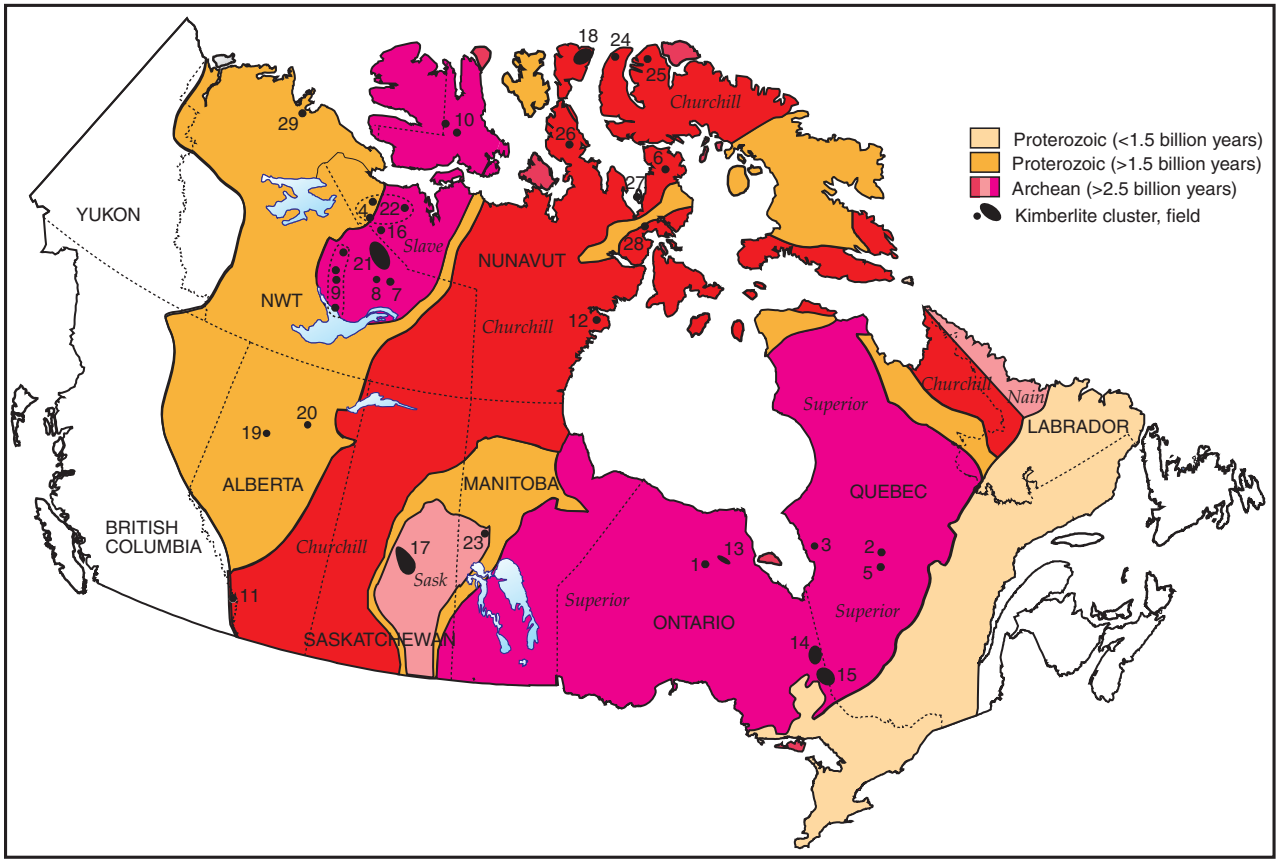

Figure 8. Distribution of Canadian kimberlites fields and clusters with respect to Proterozoic and Archean terranes (younger sedimentary cover sequences removed). The Archean Slave, Superior, Sask, Nain and Churchill cratonic blocks are shown as separate entities and labelled in italics. Localities as follows: (1) Kyle Lake cluster, Ontario; (2) Renard cluster - north Otish Mountains, Quebec; (3) Wemindji sills, Quebec; (4) Anuri, Nunavut; (5) Lac Beaver - south Otish Mountains, Quebec; (6) Aviat cluster, Melville Peninsula, Nunavut; (7) southeast Slave field, Gahcho Kué cluster, NWT; (8) southeast Slave field, Snap Lake area, NWT; (9) southwest Slave field, including the Drybones Bay and Upper Carp Lake clusters, NWT; (10) Victoria Island field (with four distinct clusters), Nunavut and NWT; (11) Crossing Creek cluster, southeast British Columbia; (12) Rankin Inlet field, Nunavut; (13) Attawapiskat field, Ontario; (14) Kirkland Lake field, Ontario; (15) Lake Timiskaming field, Ontario and Quebec; (16) Jericho cluster, Nunavut; (17) Fort à la Corne field (with six distinct clusters), Saskatchewan; (18) Somerset Island field, Nunavut; (19) Buffalo Head Hills field, Alberta; (20) Birch Mountains cluster, Alberta; (21) Lac de Gras field, NWT; (22) Coronation Gulf field, Nunavut; (23) Snow Lake - Wekusko, Manitoba; (24) Brodeur Peninsula cluster, Nunavut; (25) Baffin Island, Nunavut; (26) Boothia Peninsula, Nunavut; (27) Wales Island, Nunavut; (28) Repulse Bay cluster, Nunavut; (29) Darnley Bay cluster, NWT. Adapted from Kjarsgaard and Levinson (2002).

within the Lac de Gras field associated with the Ekati and Diavik mines.

Kimberlite Fields of Canada

Age and Geographic Distribution

Mitchell (1986) defined kimberlites as belonging to clusters, fields, and provinces. Individual kimberlite bodies grouped together are termed clusters (e.g., the Jericho cluster, Nunavut). A number of clusters within an area constitute a kimberlite field (e.g., the Lac de Gras field, Northwest Territories). Several kimberlite fields comprise a kimberlite province (e.g., the Slave kimberlite province). Kimberlites clusters usually form over time intervals of ~1 to 5 m.y., whereas kimberlites fields usually form over time intervals of ~10 to 30 m.y. (Fig. 9). Kimberlites within a kimberlite province may have a wide span of emplacement ages. In the Slave kimberlite province there are six distinct kimberlite emplacement events (Neoproterozoic, Cambrian, Siluro-Ordovician, Permian, Jurassic, Cretaceous-Paleogene; Fig. 9) with the oldest kimberlite ~613 Ma in age and the youngest kimberlite ~45 Ma in age.

The oldest known bona fide kimberlites in Canada are the Mesoproterozoic ca. 1100 Ma occurrences in the Kyle Lake cluster of northern Ontario (Fig. 8, #1). Neoproterozoic age ca. 630 Ma age kimberlites are known in central Quebec from the northern Otish Mountains area (Renard cluster; Fig. 8, #2) and eastern James Bay (Wemindji sills; Fig. 8, #3). The Renard cluster is currently at the bulk sampling stage of exploration. In the northern Slave province (in Nunavut) there is at least one Neoproterozoic age kimberlite (Anuri, ca. 613 Ma; Fig. 8, #4). Cambrian kimberlites are also observed in central Quebec in the southern Otish Mountains area (Lac Beaver, ca. 550 Ma; Fig. 8, #5). On Melville Peninsula within the Churchill province is the Cambrian age ca. 546 Ma Aviat kimberlite (Fig. 8, #6). The southeast Slave field (NWT) contains two economically important clusters of Cambrian age kimberlites, the Gahcho Kué pipes (5034 pipe, 542 Ma; Fig. 8, #7) and the Snap Lake sill (ca. 535 Ma; Fig. 8, #8). The southwest Slave field (in the NWT) contains a number of Siluro-Ordovician kimberlites dated at 463 to 435 Ma (Fig. 8, #9). Permian age kimberlites are known from Victoria Island (Fig. 8, #10).

Consistent with worldwide kimberlite emplacement age data, the majority of Canadian kimberlites are Mesozoic in age (Fig. 9). Triassic age kimberlites are rare in Canada, restricted to the Crossing Creek cluster in south-eastern British Columbia (Fig. 8, #11) and the Rankin Inlet area of Nunavut (Fig. 8, #12). There are Jurassic age kimberlites in four fields

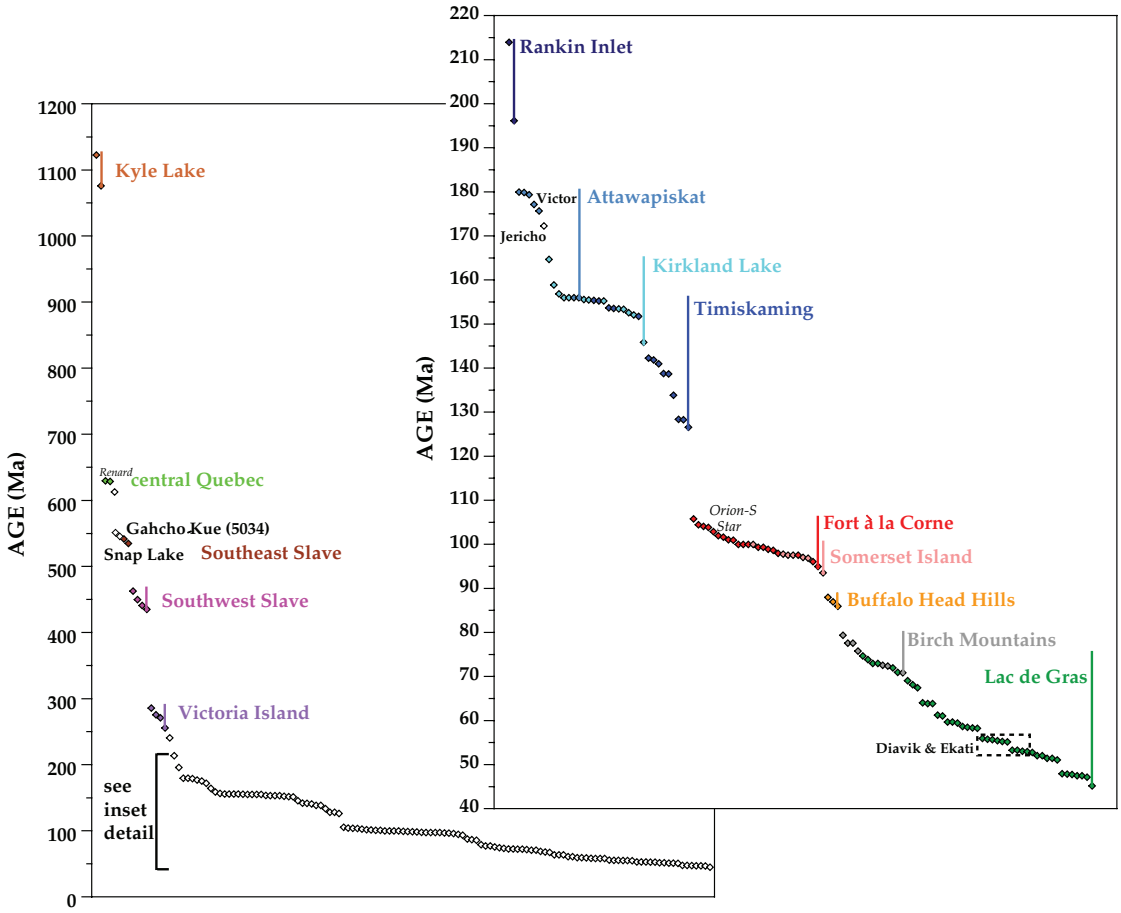

Figure 9. Detailed emplacement ages of Canadian kimberlites. Individual fields are colour coded; vertical bars denote the time span of volcanism within that kimberlite field. Data sources: Heaman and Kjarsgaard (2000); Heaman et al. (2003, 2004) and references therein; Kjarsgaard (unpublished data).

in east-central Canada, including the Rankin Inlet, Nunavut, and Attawapiskat, Kirkland Lake, and Lake Timiskaming fields, Ontario (Fig. 8, #12, 13, 14, 15, respectively). The Attawapiskat field hosts the Victor diamond mine. In the northern Slave province, Nunavut, there are also Jurassic age kimberlites, including the 172 Ma Jericho diamond mine (Fig. 8, #16). Cretaceous age kimberlites occur in east-central, central, and western Canada. The youngest kimberlites in the Lake Timiskaming field (ca. 142–126 Ma) are of Early Cretaceous age (Fig. 8 #15). Mid-Cretaceous age kimberlites occur at the Fort à la Corne, Somerset Island, and Buffalo Head Hills kimberlite fields (Fig. 8, #17, 18, 19, respectively). Late Cretaceous age kimberlites are known from the Birch Mountains (Alberta; Fig. 8, #20) and the Lac de Gras (NWT; Fig. 8, #21) kimberlite fields. The youngest kimberlites in Canada are of Paleogene age and occur in the Lac de Gras field where all the kimberlites of economic interest (Diavik and Ekati mine kimberlites) were emplaced within a narrow timespan of 56 to 53 Ma (Kjarsgaard et al., 2002).

Distribution with Respect to Geological Terranes

The majority of kimberlites in Canada (>340) are located in the Archean Slave craton, with kimberlite fields in the southeast (e.g., Snap Lake, Gahcho Kué), southwest (e.g., Carp Lake, Dry Bones Bay), central (Lac de Gras), and north Slave (Coronation Gulf; Fig. 8, #22), and on Victoria Island. In the Archean Superior province there are approximately 75 known kimberlites from the Kyle Lake, Attawapiskat, Kirkland Lake, Lake Timiskaming, Wemindji, and Otish Mountains areas (Fig. 8). The Archean Sask craton contains approximately 75 kimberlites, located in the Fort à la Corne and Candle Lake areas of Saskatchewan, and at Wekusko-Snow Lake in Manitoba (Fig. 8, #23). The Churchill province (Archean-Paleoproterozoic) hosts approximately 95 kimberlites in clusters or fields at Somerset Island, Brodeur Peninsula (Fig. 8, #24), Baffin Island (Fig. 8, #25), Boothia Peninsula (Fig. 8, #26), Melville Peninsula, Wales Island (Fig 8, #27), Repulse Bay (Fig. 8, #28), and Rankin Inlet.

More than 45 kimberlites have been discovered in northern Alberta, the majority in the Buffalo Head Hills field which is underlain by the Paleoproterozoic (2.0–2.4 Ga) Buffalo Head terrane. An additional 8 kimberlites are known from the Birch Mountains field which is underlain by the Paleoproterozoic (2.0–1.8 Ga) Taltson magmatic arc. The five kimberlites in the Crossing Creek area of southeastern B.C. are rootless, that is, they are within a thrust slice and their relationship to basement is unclear. However geological interpretations of Ross et al. (1991) suggest this area is underlain by the Hearn domain of the Churchill province. The basement terrain to the kimberlites at Darnley Bay (NT; Fig. 8, #29) is unknown but assumed to be Proterozoic.

Local Geological Setting

Kimberlites occur in clusters and fields; it is rare to find an isolated kimberlite. Although kimberlite fields are typically associated with the intersections of major structures, in detail individual kimberlites are often located on second- or third-order splays off one of the major structures (Coopersmith, 1993). In Lac de Gras some kimberlites are found at weak points in the upper crust, such as geological contacts, for example, at granite-greywacke contacts or at the margins of diabase dyke-host rock contacts (Kjarsgaard et al., 2002; Lockhart et al., 2004). In the Lac de Gras field, kimberlites of a limited age range are aligned along specific structural trends (Kjarsgaard et al., 2002). For example the economically viable (53–56 Ma) kimberlites are all within a corridor coincident with the 010º trending Lac de Gras diabase dyke swarm (Wilkinson et al., 2001; Stubley, 2004). In more detail, Lockhart et al. (2004) noted a rotation of structural alignment trends of kimberlites in the Lac de Gras field with time, starting with an ~015º trend at 55 Ma, then ~025º at 53 Ma, and ~045º trend at 48 Ma. These data are consistent with different second- or third-order crustal structures being re-activated over a 7 m.y. time period (related to far-field Cordilleran tectonics).

Deposit Scale Attributes of Kimberlites

Kimberlite Mineralogy

Kimberlite exhibits a distinctive inequigranular texture due to the presence of macrocrysts (large 0.5–10 mm rounded to anhedral crystals, typically olivine) set in a fine-grained matrix (Mitchell, 1986). Macrocryst is a non-genetic term for large crystals that could be xenocrysts, or megacrysts. Xenocrysts observed in kimberlite are composed of the following minerals: forsterite, Cr-pyrope garnet, chromian spinels, Cr-diopside, bronzite, amphibole and phlogopite from disaggregated mantle peridotite; almandine-pyrope garnet and omphacite from disaggregated mantle eclogite. Megacrysts observed in kimberlite include Ti-Cr-pyrope, Mg-ilmenite, Cr-diopside, phlogopite, enstatite, and zircon, and are thought to be high-pressure cognate phases of the kimberlite (Mitchell, 1986; Nowell et al., 2004). Primary kimberlite phenocryst/microphenocryst phases include forsterite, spinel, and more rarely phlogopite. The kimberlite groundmass consists of variable proportions of forsterite, spinels, perovskite, monticellite, apatite, phlogopite-kinoshitalite mica, carbonates, and ilmenite, although not all of these groundmass phases occur in any kimberlite. Auto-deuteric serpentine ± diopside ± calcite ± magnetite alteration of macrocrysts and primary mineral phases is common in these rocks, and typically occurs at subsolidus (<800ºC) temperatures (Wilson et al., 2007). Deuteric microcrystalline diopside with serpentine is common in crustally contaminated massive volcaniclastic kimberlite in pipes. Stripp et al. (2006) utilized thermodynamic criteria to calculate that diopside + lizardite formed at <380ºC and low pCO_2, that is, subsolidus conditions.

Kimberlite Geochemistry

Kimberlites have a characteristic geochemical signature, being rich in the incompatible elements Sr, Ba, LREE (La, Ce, Sm, Nd), Nb, Ta, Zr, P, Th, and U ('alkaline signature'), as well as having high concentrations of the first-order transition elements Mg, Ni, Cr, and Co ('ultramafic signature'). There are essentially no other rocks that have this distinctive alkaline and ultramafic geochemical signature, with the ex-

ception of a few rare magnesio-carbonatites. Some ultramafic lamprophyres (e.g., alnöite, aillikite) may also display a 'similar' geochemistry but typically these rocks have higher contents of TiO_2, Al_2O_3, Na_2O and K_2O, and can also be identified petrographically (e.g., see Tappe et al., 2005). It has been recently demonstrated by Grunsky and Kjarsgaard (2007) that it is feasible to use whole rock major-and trace-element geochemistry to distinguish and separate individual eruptive phases within a kimberlite body.

Alteration Mineralogy

At the time of intrusion or eruption, some of the kimberlite macrocryst and primary groundmass minerals may be partially or completely replaced by deuteric serpentine ± diopside ± calcite ± magnetite (see section above on kimberlite mineralogy). Furthermore, the porous nature of volcaniclastic kimberlite makes these rocks highly susceptible to post-emplacement alteration by weathering processes that cause the development clay-rich kimberlite, commonly referred to in older South African literature as "yellow" or "blue" ground.

Kimberlite Nomenclature

Kimberlites worldwide typically form small (almost always <1000 m diameter; ~80 ha) bodies (e.g., Dawson, 1980; Mitchell, 1986). The variety of shapes and sizes of kimberlites in Canada is exceptional and many of the Canadian examples do not resemble the classic South African model of a kimberlite pipe (Hawthorne, 1975). This model (Fig. 10) was constructed by utilizing the upper portion of a kimberlite pipe from Orapa, Botswana (to which a tuff ring was added) and the lower portion of a kimberlite pipe from the Kimberley area of South Africa (where 1400 m of erosion was interpreted to have occurred; Hawthorne, 1975), and is considered to represent a composite model (Kjarsgaard, 2003; Gurney et al. 2005). More recently, the erosion at Kimberley has been estimated at <850 m (Hansom et al., 2006).

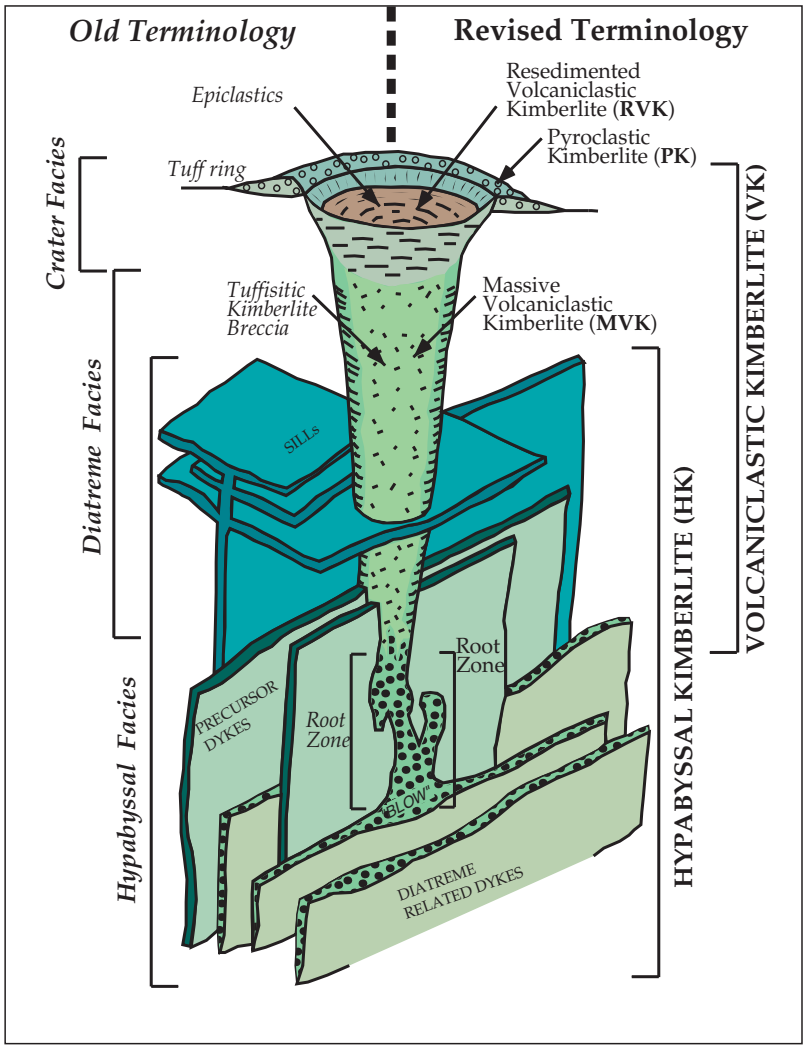

Figure 10. The classic South African model of a kimberlite pipe with old nomenclature (left side of figure) and a simpler, revised two-fold nomenclature system (right side of figure) to describe rocks from kimberlite magmatic systems (Mitchell, 1995; Kjarsgaard, 2003; Sparks et al., 2006). PK = pyroclastic kimberlite; RVK = resedimented volcaniclastic kimberlite; MVK = massive volcaniclastic kimberlite; HK = hypabyssal kimberlite. Figure modified after Kjarsgaard, 2003).

Rock types in the classic South African model were assigned to different zones or facies (e.g., Clement, 1975; Dawson, 1980; Clement and Skinner, 1985; Mitchell, 1986, 1995) which included crater facies, diatreme facies, and hypabyssal facies (Fig. 10). The use of the term facies (*the aspect, appearance, and characteristics of a rock, usually reflecting the* ***conditions*** *of its origin*), however, is incorrectly applied because the conditions of origin of diatreme facies and crater facies rocks is highly controversial (compare Mitchell, 1986 with Clement and Reid, 1989, with Lorenz et al., 1999). A simpler, non-genetic, two-fold nomenclature system (Mitchell, 1995; Kjarsgaard, 2003; Sparks et al., 2006) to describe rocks from kimberlite magmatic systems is preferred: volcaniclastic kimberlite (VK), or fragmental rocks, and; hypabyssal kimberlite (HK), or, non-fragmental rocks. The volcaniclastic kimberlites can be subdivided further into pyroclastic kimberlite (PK), re-sedimented volcaniclastic kimberlite (RVK), and massive volcaniclastic kimberlite (MVK). Note also the existence of different sub-types of PK, RVK, and MVK; different RVK subtypes include grain flow deposits and mass flow slumps. The revised terminology is shown in Figure 10 (right side), where it can be compared to the old terminology

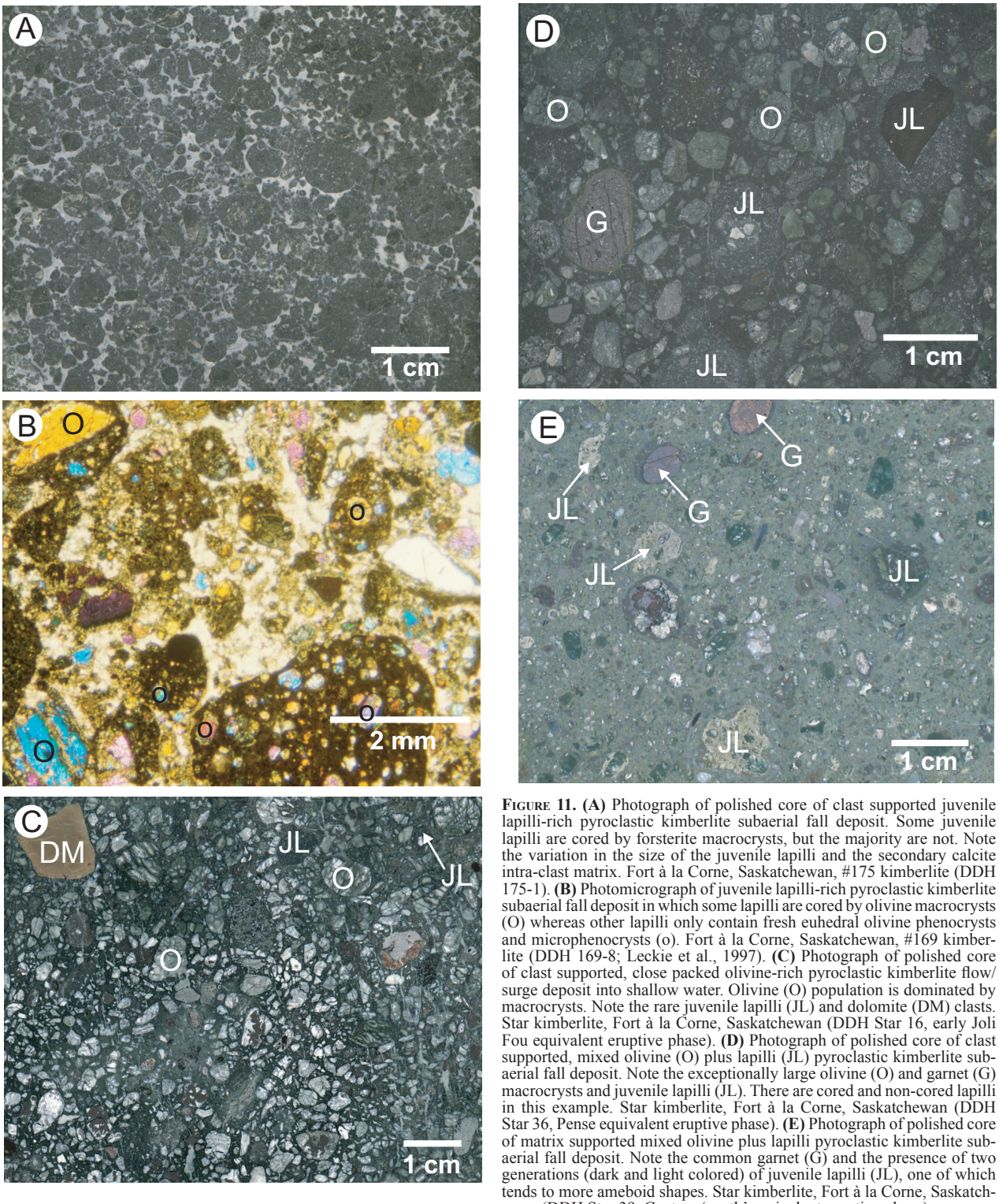

Figure 11. (A) Photograph of polished core of clast supported juvenile lapilli-rich pyroclastic kimberlite subaerial fall deposit. Some juvenile lapilli are cored by forsterite macrocrysts, but the majority are not. Note the variation in the size of the juvenile lapilli and the secondary calcite intra-clast matrix. Fort à la Corne, Saskatchewan, #175 kimberlite (DDH 175-1). **(B)** Photomicrograph of juvenile lapilli-rich pyroclastic kimberlite subaerial fall deposit in which some lapilli are cored by olivine macrocrysts (O) whereas other lapilli only contain fresh euhedral olivine phenocrysts and microphenocrysts (o). Fort à la Corne, Saskatchewan, #169 kimberlite (DDH 169-8; Leckie et al., 1997). **(C)** Photograph of polished core of clast supported, close packed olivine-rich pyroclastic kimberlite flow/surge deposit into shallow water. Olivine (O) population is dominated by macrocrysts. Note the rare juvenile lapilli (JL) and dolomite (DM) clasts. Star kimberlite, Fort à la Corne, Saskatchewan (DDH Star 16, early Joli Fou equivalent eruptive phase). **(D)** Photograph of polished core of clast supported, mixed olivine (O) plus lapilli (JL) pyroclastic kimberlite subaerial fall deposit. Note the exceptionally large olivine (O) and garnet (G) macrocrysts and juvenile lapilli (JL). There are cored and non-cored lapilli in this example. Star kimberlite, Fort à la Corne, Saskatchewan (DDH Star 36, Pense equivalent eruptive phase). **(E)** Photograph of polished core of matrix supported mixed olivine plus lapilli pyroclastic kimberlite subaerial fall deposit. Note the common garnet (G) and the presence of two generations (dark and light colored) of juvenile lapilli (JL), one of which tends to more ameboid shapes. Star kimberlite, Fort à la Corne, Saskatchewan (DDH Star 39, Cantuar 'north' equivalent eruptive phase).

(left side of Fig. 10). The revised terminology allows for a better understanding of kimberlites that do not resemble classic South African model kimberlites as more recently described by Field et al. (1997), for example, many kimberlite pipes in Canada and in other parts of the world.

Kimberlite Textures

Kimberlites are quite variable in terms of texture, although most textural features that are observed are common to other sub-volcanic systems and volcanic or volcano-sedimentary sequences. The description of these rocks, therefore, uses

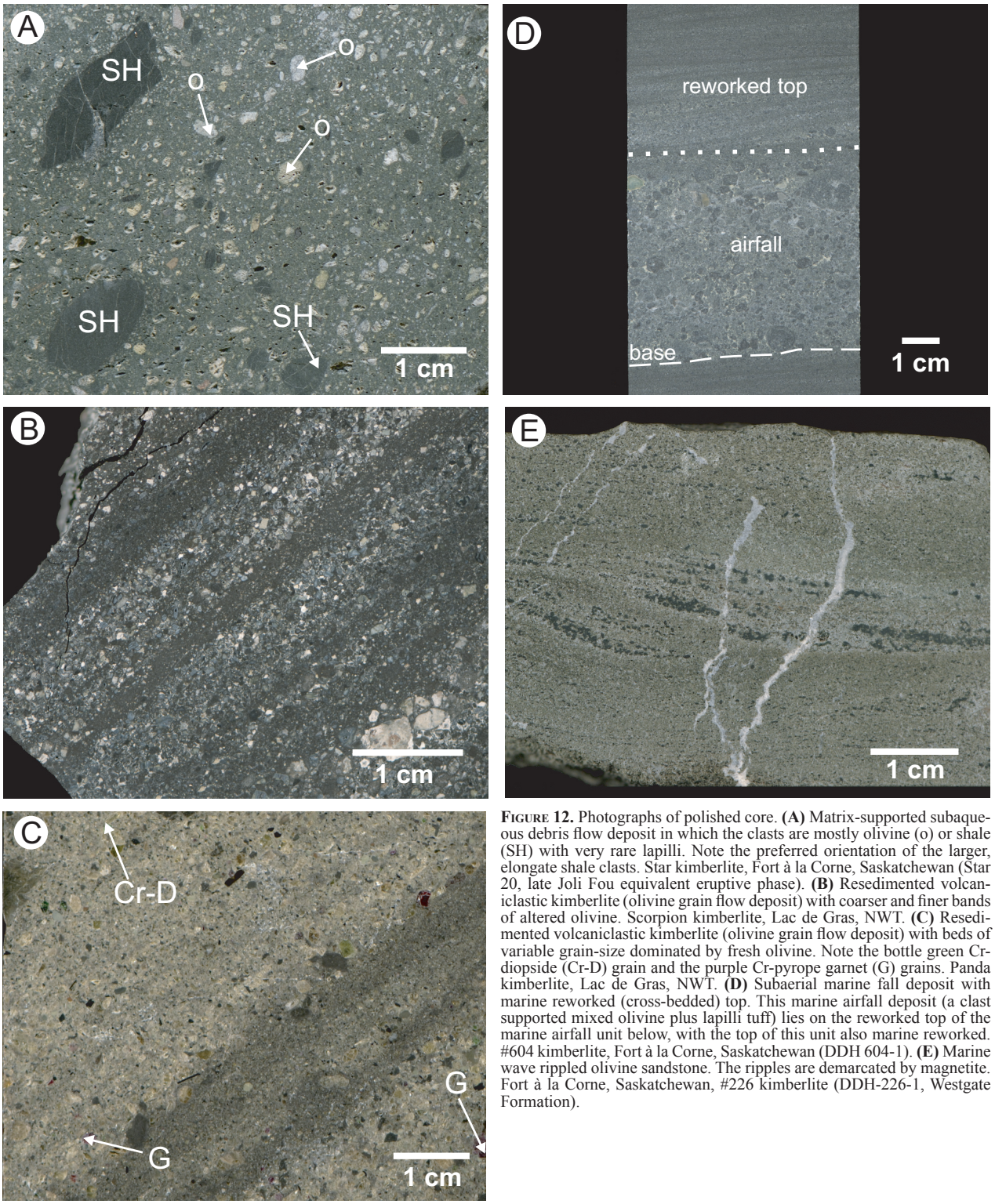

Figure 12. Photographs of polished core. **(A)** Matrix-supported subaqueous debris flow deposit in which the clasts are mostly olivine (o) or shale (SH) with very rare lapilli. Note the preferred orientation of the larger, elongate shale clasts. Star kimberlite, Fort à la Corne, Saskatchewan (Star 20, late Joli Fou equivalent eruptive phase). **(B)** Resedimented volcaniclastic kimberlite (olivine grain flow deposit) with coarser and finer bands of altered olivine. Scorpion kimberlite, Lac de Gras, NWT. **(C)** Resedimented volcaniclastic kimberlite (olivine grain flow deposit) with beds of variable grain-size dominated by fresh olivine. Note the bottle green Cr-diopside (Cr-D) grain and the purple Cr-pyrope garnet (G) grains. Panda kimberlite, Lac de Gras, NWT. **(D)** Subaerial marine fall deposit with marine reworked (cross-bedded) top. This marine airfall deposit (a clast supported mixed olivine plus lapilli tuff) lies on the reworked top of the marine airfall unit below, with the top of this unit also marine reworked. #604 kimberlite, Fort à la Corne, Saskatchewan (DDH 604-1). **(E)** Marine wave rippled olivine sandstone. The ripples are demarcated by magnetite. Fort à la Corne, Saskatchewan, #226 kimberlite (DDH-226-1, Westgate Formation).

standard volcanic or sedimentary terminology. However hypabyssal (sub-volcanic) kimberlite lithologies with numerous large forsterite crystals are not termed porphyritic, but macrocrystic as many of the large forsterite crystals are xenocrysts and not phenocrysts.

Volcaniclastic (i.e., fragmental) kimberlite (VK) is exceptionally variable in texture and is subdivided into pyroclastic kimberlite (PK), massive volcaniclastic kimberlite (MVK), and resedimented volcaniclastic kimberlite (RVK). Pyroclastic kimberlite is variable in constituent clast components, grain size, and the degree of clast support. These rocks can be clast-supported and dominated by kimberlite juvenile

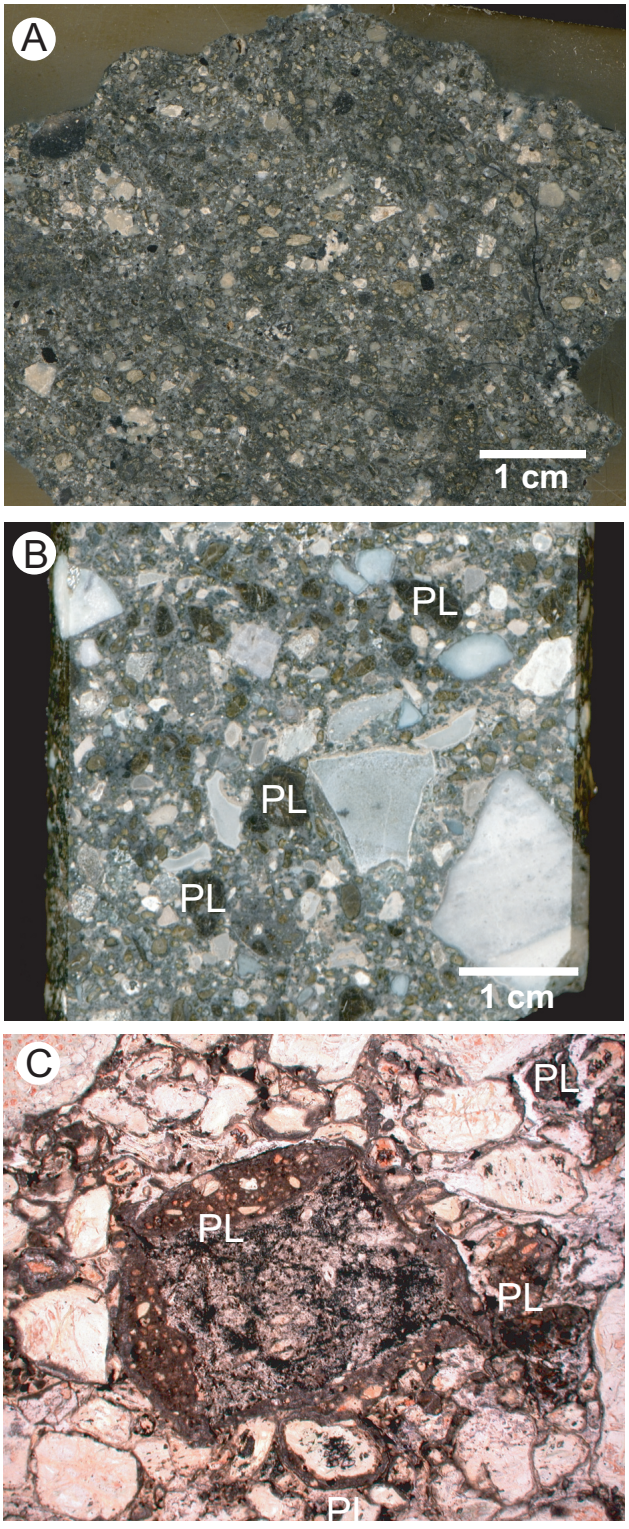

Figure 13. (A) Photograph of polished slab of massive volcaniclastic kimberlite which is relatively poor in pelletal lapilli. Fox kimberlite, Lac de Gras, NWT. **(B)** Photograph of polished core of massive volcaniclastic kimberlite breccia. Pelletal lapilli (PL) of variable size are common. Eastern "TKB". #95-2 kimberlite, New Liskeard, Ontario. **(C)** Photomicrograph of pelletal lapilli (PL) in massive volcaniclastic kimberlite breccia from the Eastern "TKB". #95-2 kimberlite, New Liskeard, Ontario.

lapilli (Fig. 11a,b), or forsterite crystals (Fig. 11c), or mixed clast assemblages of kimberlite juvenile lapilli and forsterite crystals (Fig. 11d). Matrix-supported pyroclastic kimberlite air fall deposits commonly have sub-equal clast proportions of juvenile lapilli and olivine crystals (Fig. 11e), although finer-grained matrix-supported olivine crystal tuffs are known. Base surge deposits and a variety of deposit types from primary subaerial and subaqueous (Fig. 12a) debris flows are associated with kimberlite volcanic sequences (e.g., Zonneveld et al., 2004, 2006; Kjarsgaard et al., 2005, 2006; Harvey et al., 2006).

The resedimentation of volcaniclastic kimberlite tephra results in the formation of volcano-sedimentary deposits (RVK). In the Lac de Gras kimberlite field, many of the kimberlite pipes are in-filled with forsterite-rich grain-flow (talus fan) deposits (Fig. 12b,c) and slumps. Slump deposits in the Fort à la Corne field occur as both extra-crater and, more rarely, intra-crater kimberlite deposits (Zonneveld et al., 2004, 2006; Kjarsgaard et al., 2006). Marine (Fig. 12d, e) and fluvial reworked kimberlite deposits are also common in Fort à la Corne (Leckie et al., 1997, Nixon and Leahy, 1997, Zonneveld et al., 2004, 2006).

Massive volcaniclastic kimberlite (MVK), although heterogeneous at the mm to cm scale (Fig. 13a), is often relatively homogenous at the 10 to 100 cm scale. These massive kimberlite rocks, which can occupy much of the pipe zone in the classic South African model are commonly breccias (Fig. 13b). A hallmark of these MVK rocks is the occurrence of pelletal lapilli (Fig. 13c; compare with Fig. 11b) which are discrete, spherical to elliptical lapilli-sized (2–64 mm) clasts consisting of fine-grained primary kimberlite magma (Clement, 1982; Mitchell, 1986, 1995). The centres of the lapilli are typically cored by a forsterite grain that is mantled by fine-grained to cryptocrystalline kimberlite groundmass minerals (e.g., spinel, perovskite, calcite, apatite), which are commonly oriented around the core, giving a weak to well-developed concentric structure. The replacement of the MVK groundmass by serpentine, calcite and microcrystalline diopside at subsolidus temperatures (Sparks et al., 2006, Stripp et al., 2006) leads to the development of the distinctive (but inappropriately named) tuffisitic kimberlite breccia (TKB) first described at numerous southern African kimberlite occurrences.

Hypabyssal kimberlite (HK) commonly exhibits a distinctive inequigranular texture due to the presence of large, rounded, anhedral macrocrysts (i.e., megacrysts and xenocrysts) plus euhedral to subhedral phenocrysts set in a finer-grained groundmass (Fig. 14a,b). HK breccias contain abundant country rock clasts (Fig. 14c). The HK groundmass is either uniform in appearance or contains segregations of auto-deuteric calcite +/- serpentine. Mitchell (1986, 1997) provides numerous excellent photomicrographs of uniform and segregation textured HK. Flow banding (or flowage differentiation) is a well-documented igneous process in basic sills and dykes (Bhattacharji and Smith, 1964; Drever and Johnston, 1966) that is also observed in kimberlites (Figs. 14d, 15a). Crystal settling appears to be a rare process (Fig. 15b) in kimberlite magmatic systems, but has been observed at the Benfontein sill in South Africa (Dawson and Hawthorne,

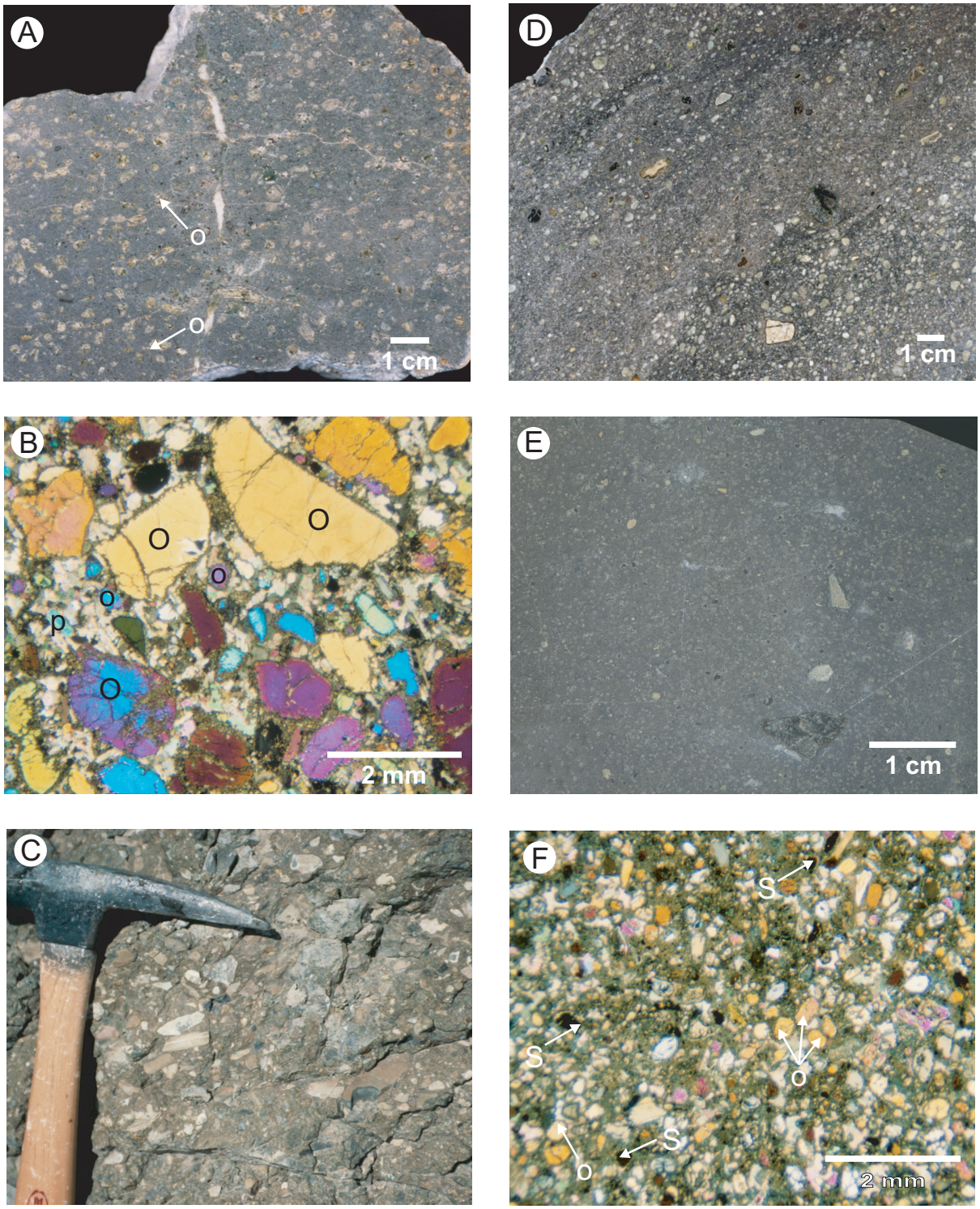

Figure 14. **(A)** Photograph of polished slab of hypabyssal macrocrystic kimberlite. Note the fresh olivine macrocrysts (O) and the secondary calcite veinlets (white, centre field of view). K4 kimberlite, Somerset Island, Nunavut. **(B)** Photomicrograph of hypabyssal macrocrystic kimberlite with fresh anhedral to subhedral olivine macrocrysts (O), subhedral to euhedral olivine phenocrysts (o), rare phlogopite (p) and spinel phenocrysts. Groundmass is dominated by calcite (tabular and subhedral). Brown turbid areas are groundmass (spinel + serpentine + carbonate + apatite) not resolvable at the scale of the photomicrograph. Jos kimberlite dyke, Somerset Island, Nunavut. **(C)** Photograph of hypabyssal kimberlite breccia outcrop near the margin of the intrusion. Country rock clasts are dominated by the local host rocks (limestone and dolostone). K-20 kimberlite, Somerset Island, Nunavut. **(D)** Photograph of polished slab of flow banded hypabyssal macrocrystic kimberlite, with alternating bands of coarser and finer olivine grains. Peddie kimberlite, New Liskeard, Ontario. **(E)** Photomicrograph of aphanitic hypabyssal kimberlite. Note that with the exception of rare, larger country rock clasts, the sample could easily be confused as a basalt from a purely macroscopic perspective, due to the absence of any olivine macrocrysts and the abundant olivine (o) phenocrysts and microphenocrysts. McLean kimberlite, New Liskeard, Ontario. **(F)** Photomicrograph of aphanitic hypabyssal kimberlite. Note the sample consists of essentially sub-equal amounts of euhedral to subhedral olivine (o) plus minor spinel (s) phenocrysts and groundmass (spinel + serpentine + carbonate + apatite) not resolvable at the scale of the photomicrograph. Peuyuk kimberlite, sub-phase of intrusion "A", Somerset Island, Nunavut.

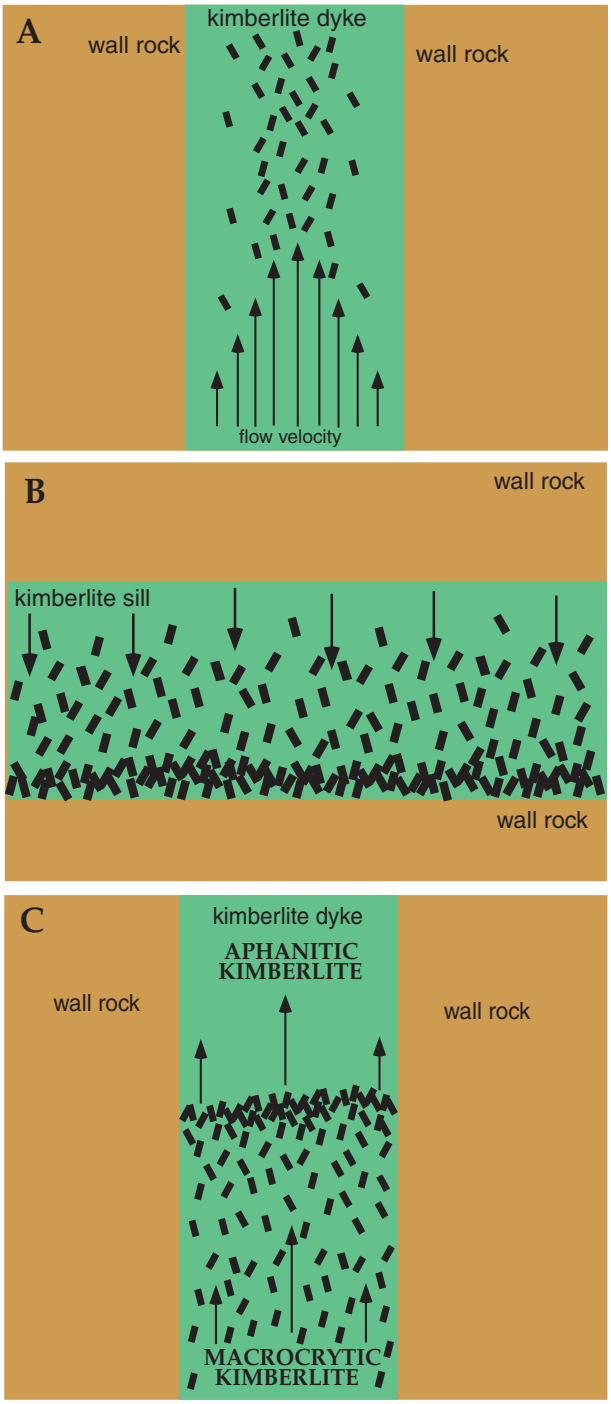

Figure 15. (A) Schematic representation of flow banding in a kimberlite dyke, with increased flow rates at the centre due to dispersive shear pressure. **(B)** Schematic representation of gravitational crystal settling (magmatic sedimentation) in a kimberlite sill. **(C)** Schematic representation of filter pressing in a kimberlite dyke (all figures adapted from Kjarsgaard, 2003).

1973). Filter pressing in dykes, sills, or plugs (Fig. 15c) and flowage differentiation processes can lead to the formation of aphanitic kimberlite as observed at the McLean and Peuyuk kimberlites (Fig. 14e, f) and the Jericho kimberlite (Price et al., 2000).

Architecture and Morphology of Kimberlites

Shape and area of kimberlite bodies: Kimberlite pyroclastic rocks and volcaniclastic deposits that form volcanic edifices (tephra cones, tuff cones, tuff rings) are not common due to their low preservation (typically <1 m.y.), but do occur in Mali, Tanzania, and Canada (Kjarsgaard, 2007). The best-preserved volcanic edifices in the world are found at the Fort à la Corne kimberlite field, Saskatchewan, and at the Buffalo Head Hills kimberlite field, Alberta. In Saskatchewan, individual volcanic phases have up to ~100 m of preserved relief above the paleo-eruptive surface and are up to ~900 m in diameter (Kjarsgaard, 2007). Fort à la Corne kimberlites with multiple feeder vents have coalesced tephra cones and/or rings, and can form much larger bodies up to 2.5 km diameter (Fig. 16). These feeder vents are quite variable in their morphology, ranging from narrow pipe-like bodies to wider flared vents (Fig. 16), and can be infilled by MVK, VK, and PK (Kjarsgaard et al., 2004, 2006; Harvey et al, 2006). Kimberlites from the Buffalo Head Hills field (Carlson et al., 1999) have some basic similarities to those of Fort à la Corne with regard to kimberlite body geometry, but in detail some slightly different pyroclastic rock types are present (e.g., accretionary lapilli tuffs; Boyer, 2005). Although no kimberlite lava lakes have been identified, large HK bodies in the Lac de Gras area (Nowicki et al., 2007) have been tentatively interpreted as welded spatter deposits. If true, these deposits must have formed from Hawaiian-style fire fountaining at very high effusion rates. The lava flow at the Igwisi Hills, Tanzania could have a similar origin (S. Kurszlaukis, pers. commun., 2007).

Massive volcaniclastic kimberlite (MVK)-dominated pipes are exceptionally variable in area, ranging from ~50 to 500 m, rarely to 800 m diameter. Although they tend to be generally circular in plan view, the pipes are typically highly irregular in shape. This effect is pronounced if local faulting, fracture sets, or host-rock geology has strongly influenced the growth of the pipe during the eruptions (Barnett and Lorig, 2007). Kimberlite pipes of similar geometry to the classic South African model form carrot-shaped pipes (Fig. 10) typically infilled by HK, MVK, and RVK (e.g., Fig. 17 a–c). Examples of this type of pipe in Canada include several kimberlites in the Kirkland Lake and Lake Timiskaming fields, Ontario, and at some kimberlite pipes in the North Slave field (NWT), plus the Fox and Nicholas Bay kimberlites in the Lac de Gras area. The best described example of a pipe dominated by MVK and RVK is at Orapa, Botswana (Field et al., 1997).

The kimberlite pipes in the Lac de Gras field tend to be quite small (50–150 m diameter; <5 ha), steep sided (Fig. 18), and highly irregular (Graham et al., 1999; Nowicki et al., 2003). The pipe infill is in some cases dominated by kimberlite slumps and grain flows resedimented from a pyroclastic tephra cone (Fig. 19; Kjarsgaard, 2003, 2007) that formed during the pipe excavation stage. At Lac de Gras, consequent or subsequent input of pyroclastic kimberlite also contributes to the pipe infill (e.g., Kirkley et al. 1998; Graham et al., 1999; Moss and Russell, 2006). Canadian examples of pipes infilled with resedimented volcaniclastic kimberlite include

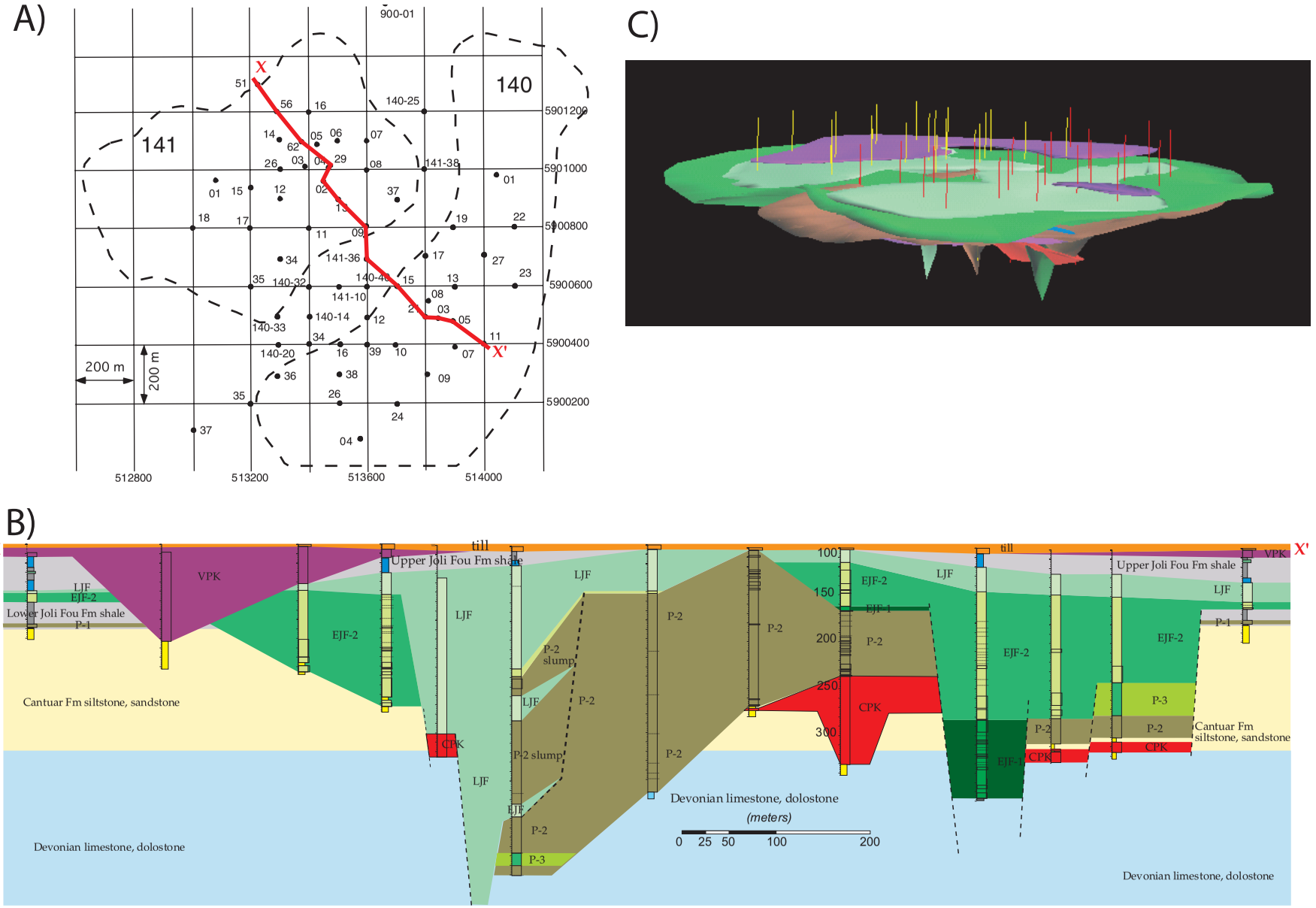

Figure 16. (A) Plan view of Orion South (140/141) kimberlite, Fort à la Corne field, Saskatchewan. Line of cross section X–X' shown in red. **(B)** Northwest–southest cross section of the Orion South (140/141) kimberlite, 1:1 scale, no vertical exaggeration. Seven distinct eruptive phases are identified in this model: purple = VPK; light green = LJF; green = EJF-1; dark green = EJF-1; brown = P-2; lime green = P-3; red = CPK. One minor phase also shown in brown = P-1. Note that four distinct feeder vents are identified (CPK, EJF-1, P-2, LJF). **(C)** 3-D solids model of the Orion South kimberlite illustrating relationships between the major eruptive phases and their feeder vents. Modified after Harvey et al., (2004).

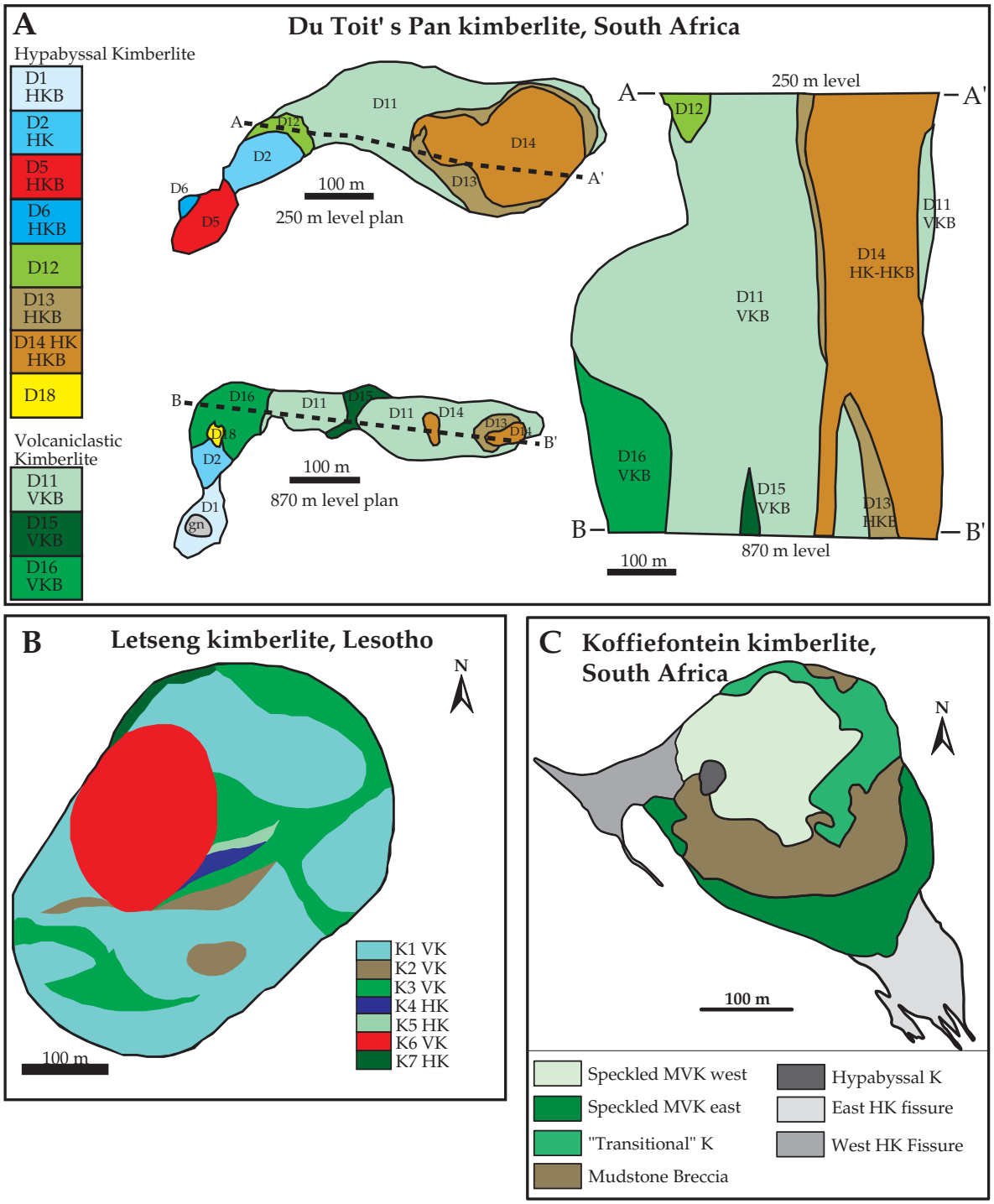

Figure 17. **(A)** Plan views of the 250 m and 870 m levels of the Du Toit's Pan, South Africa kimberlite and section view from the 250 m to 870 m level (after Clement, 1982). **(B)** Plan view of the Letseng, Lesotho kimberlite (after Bloomer and Nixon, 1973). **(C)** Plan view of the Koffiefontein, South Africa kimberlite (after Naidoo et al., 2004). Note that for each kimberlite the multiple varieties of distinct kimberlite identified.

the Panda, Koala, Misery, A-154N, and A-154S pipes.

Hypabyssal kimberlite dykes and sills are typically from 0.1 to 3 m in width (or thickness), and rarely to 5 to 10 m. Dyke enlargements (blows) and plugs of hypabyssal kimberlite range up to 100 m in diameter, and individual dykes or sills may be traced discontinuously (bifurcating with en echelon offsets being typical, as is common for basaltic dyke or sill systems) from a few hundred metres up to a few kilometres. The Snap Lake (NWT) kimberlite sill (Kirkley et al., 2003), the Somerset Island K24 kimberlite dyke (Kjarsgaard, 1996), and the Lynx dyke in the Otish mountains, Quebec, are good examples of spatially extensive (>1 km) kimberlite bodies.

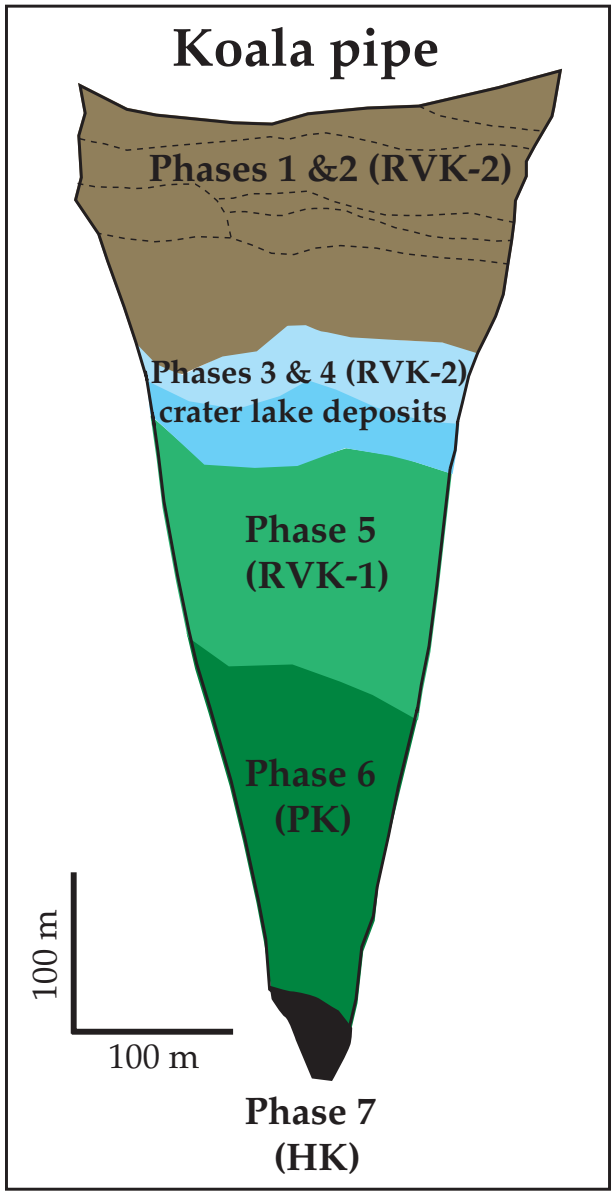

Figure 18. Geological cross section of the steep-sided, inverted cone shaped Koala kimberlite body, Ekati Mine, Lac de Gras field. Phase 7 is hypabyssal kimberlite (HK) and Phase 6 is pyroclastic kimberlite (PK) (Crawford et al., 2006). Phase 5 is interpreted here as syn-eruption resedimented volcaniclastic kimberlite (RVK-1); phase 4 and 3 are interpreted here as crater lake sediment;, and phases 2 and 1 are interpreted as post-eruption resedimented volcaniclastic kimberlite (RVK-2). Internal phases within phase 1 and 2 demarcated by dashed lines. Modified after Nowicki et al. (2003) and Crawford et al., (2006).

Irregularly shaped, multiple-lobed root zone complexes consisting dominantly of hypabyssal kimberlite have been observed at the Renard kimberlites, Québec, and the Batty Bay complex, Somerset Island, Nunavut. Massive, plug-like bodies of hypabyssal kimberlite have also been observed at the Notre Dame du Nord (NDN) and Peddie kimberlites in the Lake Timiskaming fields, Ontario.

The Multiphase Intrusive–Extrusive Nature of Kimberlite Bodies: Of crucial importance in understanding the diamond potential of a kimberlite is the recognition that multiple intrusive (HK, MVK) and/or extrusive (MVK, VK, PK) kimberlite phases occur within a single kimberlite body (Figs. 5, 16, 17, 18). Previous (e.g., 1970s, 1980s, 1990s) and also some current (i.e., 2006) geologic and genetic models for the formation of kimberlite pipes are oversimplified. For example, the conceptual classic South African model (Figs. 10, 20c) shows only a simple stratification of rock types, with PK and RVK at the top of the pipe, the pipe infilled by MVK, and HK in the root zone at the base of the pipe. This is not in accord with geological observations (e.g., Moulle, 1885, Wagner, 1914; Nixon, 1973; Clement, 1982). For example, at the Du Toit's Pan (South Africa) kimberlite (Fig. 17a), the upper part of the pipe (the 250 m level) is occupied by one MVK phase and six different HK phases. At the Letseng (Lesotho) kimberlite (Fig. 17b), the upper part of the pipe is occupied by four different MVK phases and three different HK phases. The Koffiefontein (South Africa) kimberlite (Fig. 17c) pipe on the 470 m level is occupied by two different MVK phases, two RVK phases, and three different HK phases. Taken together, the geological observations from three different classic South African model kimberlite pipes are consistent with the idea of multiple kimberlite phases in a single pipe as originally suggested by Moulle (1885) and Wagner (1914). Although Clement and Reid (1989) did note that HK and MVK are observed at the same structural level within a pipe, the models illustrated in Figures 10 and 20 show a simple stratification of different kimberlite rock types with depth in contrast to what is actually observed.

Simplified geologic models constructed for kimberlites from the Fort à la Corne and Lac de Gras area (Field and Scott-Smith, 1999; Scott-Smith, 2006) are illustrated in Figures 20a,b. These models serve little, if any purpose, because they are so oversimplified that they are misleading with respect to the known variation in architecture and morphology, internal geology (i.e., the multiple intrusive/eruptive nature of kimberlites), and hence diamond economics. For example, see Harvey et al. (2006), Kjarsgaard et al. (2006), or Kjarsgaard (2007) for Fort à la Corne kimberlites and Nowicki et al. (2003), Crawford et al. (2006), or Moss and Russell (2006) for Lac de Gras kimberlites.

Genetic and Exploration Models

Conventional Models

Diamonds have formed over a significant period of Earth history, from ~3.57 Ga (Gurney et al., 2005) to 88 Ma (Pearson and Shirey, 2002), and are represented by many diamond forming events (Shirey et al., 2004; Gurney et al., 2005). Diamonds are interpreted to crystallize from low-density fluids, or carbon- and water-rich melts (Bulanova, 1995; Navon, 1999). Macro-diamonds are transported as xenocrysts from the mantle to the surface by kimberlite magmas. Kimberlite-hosted diamond mines occur in a restricted tectonic setting and are observed only in ancient continental shield regions (Clifford, 1966) older than 2.5 Ga (Janse, 1984). The most favourable tectonic environment for economic kimberlites is a thick, old (2.5–3.6 Ga) craton with low heat flow. The kimberlite magmatism is initiated at depth in the mantle (>150 km),

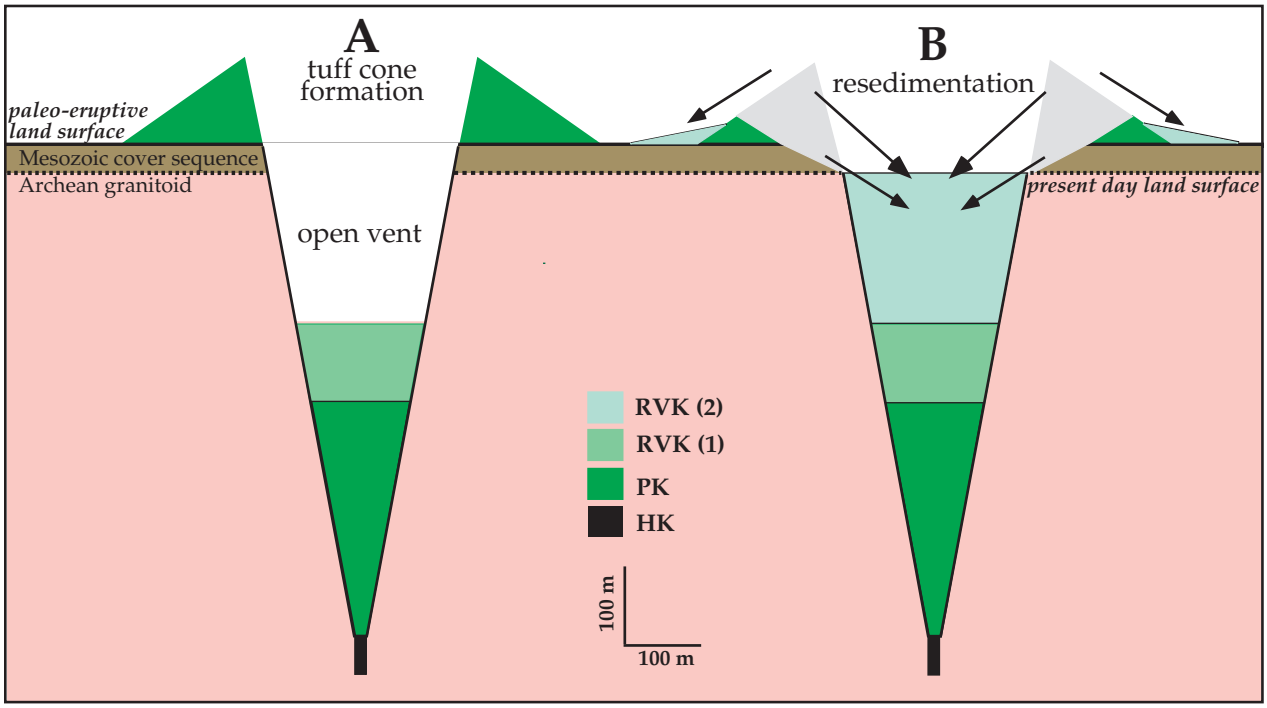

Figure 19. (A) Scaled model for the reconstruction of a kimberlite tephra cone at the Koala pipe, NWT. The tephra cone is 600 m in diameter and 108 m high with a crater rim diameter of 300 m an angle of repose of ~36°, and an internal crater wall angle of ~78°. The tephra cone sits on a 32 m thick Mesozoic cover sequence, on top of Archean granitoids. **(B)** Resedimentation of kimberlite (from the tephra cone) and cover sequence sediments by grain flow and slumping processes, into the open excavated pipe. The model assumes it is not feasible for the entire tephra cone to be resedimented into the open pipe, i.e., tephra will also be displaced away from the open pipe. 1:1 scale, no vertical exaggeration. Adapted and modified after Kjarsgaard (2003, 2007)

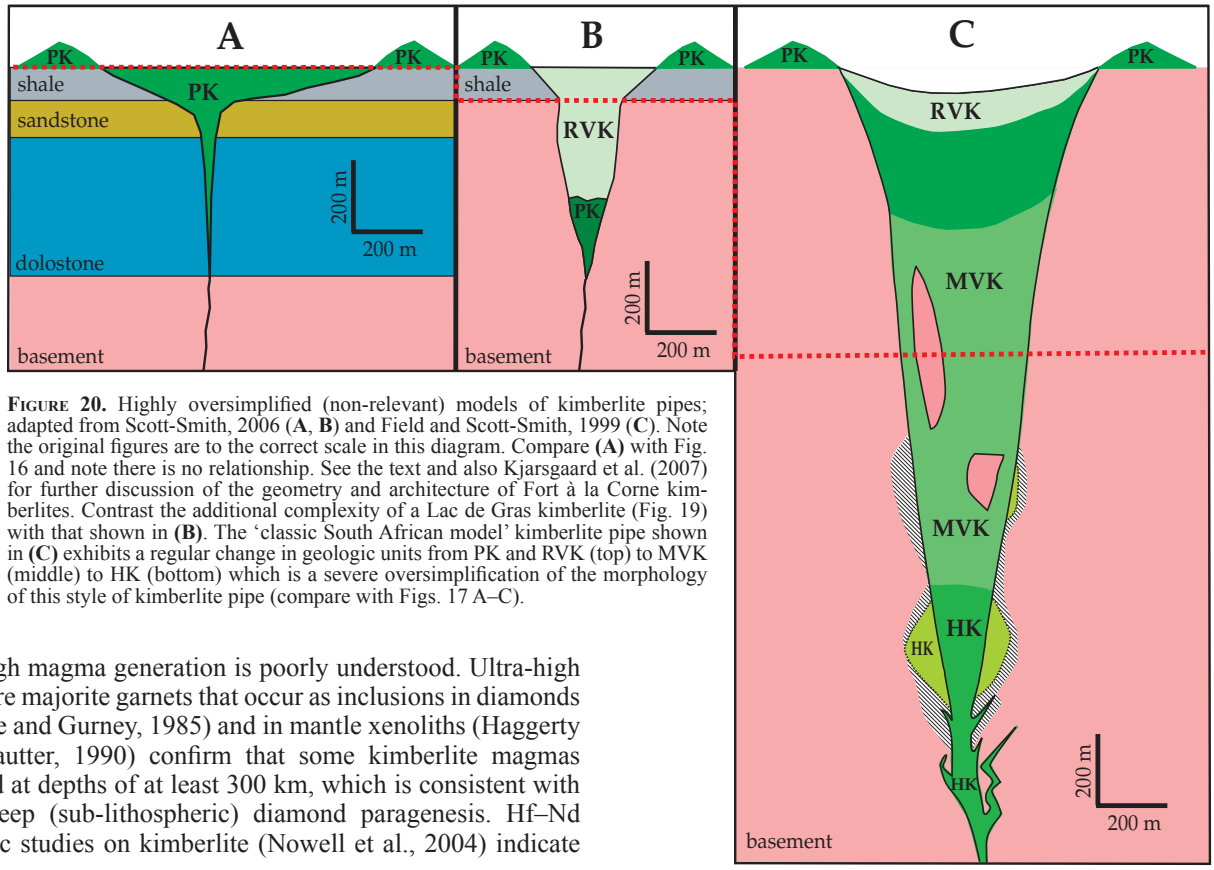

Figure 20. Highly oversimplified (non-relevant) models of kimberlite pipes; adapted from Scott-Smith, 2006 (**A**, **B**) and Field and Scott-Smith, 1999 (**C**). Note the original figures are to the correct scale in this diagram. Compare **(A)** with Fig. 16 and note there is no relationship. See the text and also Kjarsgaard et al. (2007) for further discussion of the geometry and architecture of Fort à la Corne kimberlites. Contrast the additional complexity of a Lac de Gras kimberlite (Fig. 19) with that shown in **(B)**. The 'classic South African model' kimberlite pipe shown in **(C)** exhibits a regular change in geologic units from PK and RVK (top) to MVK (middle) to HK (bottom) which is a severe oversimplification of the morphology of this style of kimberlite pipe (compare with Figs. 17 A–C).

although magma generation is poorly understood. Ultra-high pressure majorite garnets that occur as inclusions in diamonds (Moore and Gurney, 1985) and in mantle xenoliths (Haggerty and Sautter, 1990) confirm that some kimberlite magmas formed at depths of at least 300 km, which is consistent with ultra-deep (sub-lithospheric) diamond paragenesis. Hf–Nd isotopic studies on kimberlite (Nowell et al., 2004) indicate

that the source area for kimberlite magmas resides at depth in the convecting mantle but taps an isotopic reservoir of ancient, deeply subducted basalt.

Thermobarometric calculations on mineral assemblages from diamondiferous mantle xenoliths (Pearson et al., 1994) and polymineralic diamond inclusions are consistent with diamonds forming in the Earth's mantle at depths greater than ~150 km. On the basis of petrological studies on eclogites and C isotopic studies on E-type diamonds, it is suggested that the C for many of these diamonds originated at or near the Earth's surface and was transported into the mantle via subduction processes (Jacob, 2004; Gurney et al., 2005; Jacob et al., 2005). In contrast, P-type diamonds have a very restricted range of C isotopic compositions, similar to and consistent with a juvenile (mantle) C source. The range in diamond contents of kimberlites (<.001 to >10 carat/tonne) is dependent upon the amount of diamond-bearing eclogite and peridotite lithospheric mantle material plus ultra-deep diamonds sampled, and the degree to which resorption and mechanical sorting of this entrained material occurs during transport to the surface. Kimberlites probably ascend through the mantle at velocities of 10 to 30 km/hr by crack propagation processes (Eggler, 1989). High level, rapid H_2O and CO_2 degassing coupled with groundwater interaction may result in highly explosive near-surface magmatism and the formation of kimberlite pipes, tephra cones, tuff cones, and tuff rings of variable geometry. Multiple intrusive and/or extrusive kimberlite phases are the norm, and inter- and intra-phase diamond variation may exceed an order of magnitude.

Advances of the Last Decade

There have been a number of significant advances in exploration for kimberlite-hosted diamond deposits in the past decade. The geochronology of kimberlites on a local and global scale has illustrated that eruption age is potentially important with respect to diamond prospectivity (Heaman et al., 2003, 2004). This enhanced understanding is due mainly to the development of the U–Pb perovskite radiometric technique by L. Heaman, and the Ar/Ar technique on groundmass phlogopite. A major increase in the understanding of the Earth's lithosphere has arisen due to deep seismic studies in Canada (Musacchio et al., 2004) and southern Africa (Fouch et al., 2004). These studies have been complimented by direct age dating of mantle xenoliths (e.g., Pearson et al., 1995, 2002; Carlson et al., 2000; Irvine et al., 2003). There is, however, significant scope for additional studies to be undertaken in these areas.

The development of single mineral grain thermobarometers (i.e., clinopyroxene method for peridotite derived grains; Nimis and Taylor, 2000) to understand fossil paleogeotherms and thus diamond stability is a major advance in diamond exploration, although these methods are not as precise in comparison to the more time consuming methods of traditional four- or five-phase thermobarometry. Furthermore, a thermobarometer has recently been developed for eclogite xenoliths (Simakov, 1999). Previously, it was only possible to determine eclogite paleotemperature and determine equilibration pressure by assuming a fossil geotherm (based on peridotite data) to understand if the eclogite equilibrated in the diamond or graphite stability field.

The use of garnet xenocryst data to reconstruct the lithospheric mantle in terms of the proportions of eclogite and various types of peridotite by Schulze (1989, 1994) was an important conceptual breakthrough. More recently, the concept of mantle stratigraphy has been attempted by trace element analysis of peridotite garnets (e.g., Griffin et al., 2004), combined with single grain Cr-pyrope thermobarometry on the garnets (Ryan et al., 1996). Unfortunately, these mantle stratigraphic methods do not take into account the amount of chromite harzburgite, chromite dunite, or eclogite in the mantle sample. Importantly, it has been shown by a number of authors (e.g., Gurney et al., 2005) that E-type diamonds can be an exceptionally important and sometimes the dominant component of the total (P-type, E-type, ultra-deep) diamond population within a kimberlite hosted diamond deposit.

Understanding the major element geochemistry of kimberlite indicator minerals Cr-pyrope garnet, Cr-spinel, Mg-ilmenite, and Cr-diopside has undergone a number of significant advances in the past decade. Wyatt et al. (2004) determined a new MgO versus TiO_2 bivariate plot to distinguish kimberlitic from non-kimberlitic ilmenite. Ramsay and Tompkins (1994) provided new insights on Cr-diopside parageneses applicable to diamond exploration. Grütter et al. (2004) published a simple, easy to use garnet discrimination/classification scheme, based on a large data set, using sound petrological principles. This classification allows for discrimination of wehrlite garnet (G12); high-Ti peridotite garnet (G11); harzburgite/dunite (subcalcic) garnet (G10); lherzolite (Ca-saturated) garnet (G9); pyroxenite–websterite–eclogite garnet (G4); eclogite garnet (G3); and megacryst garnet (G1).

The application of kimberlite indicator minerals as diamond indicator minerals has also significantly advanced in the past decade through the use of major- and trace-element data. In the recent Grütter et al. (2004) classification system, diamond harzburgite/dunite (subcalcic) garnet can now be discriminated on the CaO versus Cr_2O_3 bivariate plot. Furthermore, pressure is estimated from the Cr content of these peridotite-derived garnet xenocrysts (Grütter et al., 2006). For eclogite garnets, discrimination of diamond eclogite garnet is accomplished by use of a TiO2 versus Na_2O bivariate diagram (Fipke et al. 1995; Schulze, 1997). New and revised diamond Cr-spinel discrimination plots utilizing Cr_2O_3 with MgO, TiO_2, Al_2O_3 and Fe_2O_3 (e.g., Grütter and Apter, 1998; Kjarsgaard, 1998a) update the original discrimination plots of Sobolev (1971, 1977). These new and revised kimberlite indicator mineral and diamond indicator mineral plots are illustrated in McClenaghan and Kjarsgaard (2007).

A number of significant advances have occurred with regard to the application of airborne magnetic and EM surveys for kimberlite exploration. The application of GPS-controlled flight lines has certainly improved line spacing and the geographic positioning of the survey, which is particularly important for detailed surveys. The application of airborne gravity systems developed over the past decade has not (as yet) found any kimberlites of economic significance that were not previously recognized by magnetic and/or EM surveys. The development and application of seismic and MT methods to

kimberlite exploration has been limited (Ford et al., 2007), but the results thus far are encouraging (e.g., Hammer et al., 2004).

There has been a renewed recognition over the past decade that kimberlite diamond deposits are complex, multiple intrusive/extrusive bodies. Although this has been known for over 100 years, over-simplified kimberlite pipe models developed in the 1970s, 80s, and 90s (see Fig. 10), are still (2006), in part, being perpetuated (see Fig. 20), which has led to non-optimum diamond sampling strategies in some cases.

Key Exploration Criteria

Surficial Indicator Mineral and Geochemical Sampling

Kimberlites contain a distinctive suite of resistant minerals of varying abundance known as kimberlite indicator minerals (Gurney and Zweistra, 1995). These include garnets, spinels, ilmenite, clinopyroxene, forsterite, orthopyroxene, and zircon. The indicator minerals are derived from the megacryst suite, disaggregated mantle peridotite, and eclogite, and from the kimberlite itself (see previous section on kimberlite mineralogy). The use of these indicator minerals in regional and detailed glacial till, stream sediment, and soil sampling programs to explore for kimberlite is well established worldwide. McClenaghan and Kjarsgaard (2007) summarize the salient visual, mineralogical, and geochemical characteristics of these minerals as applied to kimberlite and diamond exploration.

The distinctive geochemical signature (see previous section on kimberlite geochemistry) of kimberlite forms the basis for the exploration of these deposits using the chemical composition of glacial tills, stream sediments, and soils. Note, however, that any geochemical anomalies may be of limited areal extent due to dilution of the diagnostic kimberlite signature during dispersion in till and stream sediments (see further discussion in McClenaghan and Kjarsgaard, 2007).

Geophysical Prospecting Methods

The physical properties of kimberlite are quite variable, depending upon the type of kimberlite (HK, MVK, VK, PK, RVK) and style(s) of alteration. Kimberlite bulk densities range from ~2.5 to 3.1 g/ml for non-fragmental HK, to much lower values of 1.6 to 2.5 g/ml for fragmental VK (Katsube and Kjarsgaard, 1996). Kimberlite electrical resistivity measurements range from ~3,000 to 60,000 Ωm for non-fragmental HK to much lower values of ~10 to 3,000 Ωm for fragmental VK (Katsube and Kjarsgaard, 1996). Kimberlite magnetic susceptibility ranges from ~1 to 100 (10^{-3} S.I. units) for both HK and VK (Katsube and Kjarsgaard, 1996). Because kimberlite bodies can be hosted by just about any type of rock, the physical properties of host rocks are widely variable in terms of their magnetic response, electrical resistivity, and density. Hence, kimberlites can be represented by either positive or negative anomalies on airborne or ground magnetic, electromagnetic, and gravity surveys. Furthermore, because of the protracted emplacement of kimberlites over a timespan of up 30 m.y. (Heaman and Kjarsgaard, 2000; Heaman et al., 2003, 2004), they may be represented as both positive and negative magnetic features on airborne or ground magnetic surveys due to reversal(s) of the Earth's magnetic field.

A limited number of seismic (reflection and refraction) surveys have been undertaken over kimberlites with varying results. Recent surveys in Canada have shown that this technique can be effective in delineating sills in granite greenstone terrains (e.g., Snap Lake; Hammer et al., 2004) and sediment-hosted kimberlite tephra cones/feeder vents (e.g., Buffalo Head Hills; Fort à la Corne, Gendzwill and Matieshin, 1996; Carlson et al., 1999). In Canada, the application of airborne multi-spectral (Th, U, K) radiometric surveys has not been shown thus far to be an effective kimberlite exploration tool (Richardson, 1996). However, Macnae (1995) indicated that anomalous responses have been reported for kimberlites in India and Siberia, and noted that, due to limited depth penetration of this method, it would only be useful for outcropping kimberlites. In glaciated terrains such as Canada, this technique may be effective in identifying very kimberlite-rich tills. Airborne and ground hyperspectral imaging techniques to identify alteration minerals has been shown to be effective in non-glaciated terrains (e.g., Australia), however in glaciated terrains, dilution masks or lowers the response of diagnostic target minerals (Kerr et al., 2002). Macnae (1995), Walker (2003) and Ford et al. (2007) provide excellent overviews on the applications of geophysics to kimberlite exploration.

Sampling Strategies

Because there may only be one economically viable kimberlite body within a field or cluster, every potential target needs to be identified and drilled or sampled. To delineate the number of kimberlites within a cluster or field, typically a combination of geophysical techniques (airborne and ground) coupled with indicator mineral (and boulder) sampling and/or geochemical sampling in till, stream sediments, or soil is undertaken. In areas where the kimberlite is exposed or shallowly buried, a preliminary assessment of the diamond potential can be obtained economically by sampling in pits or trenches. Coopersmith (1993) provides a good synopsis of sampling techniques for pits and trenches on exposed or shallowly buried pipes. Deeply buried deposits need to be systematically drilled to be evaluated.

After sampling drill core or pits and trenches, it is crucial to discriminate distinct kimberlite phases within samples. This is accomplished by detailed macroscopic observations coupled with whole-rock geochemistry and geophysical (magnetic, density, multi-spectral gamma) techniques on core or hand samples, or by down-hole geophysical methods. Additional detailed petrographic analysis by microscopy or microbeam methods may also be required. Sampling for diamond indicator minerals or diamonds is undertaken on the basis that discrete kimberlite phases within a kimberlite body are sampled separately. Analysis of microdiamond-size populations, with the diamonds recovered using caustic or acid dissolution techniques, utilizes a variety of statistical techniques (e.g., Rombouts, 1995; Chapman and Boxer, 2004). The analysis of diamond indicator minerals is undertaken utilizing a variety of geochemical screening criteria (see summary in Advances of the Last Decade).

Knowledge Gaps

A significant problem for diamond explorationists is recognizing and understanding the significant variability in the architecture and morphology of kimberlite bodies worldwide. Perhaps even more important is the recognition and understanding of discrete phases within an individual kimberlite body. The various factors (e.g., phreatomagmatic versus primary magmatic volatile driven) involved in the different styles of kimberlite magmatism is poorly understood at present due to an almost complete paucity of supporting data sets. Hence, basic genetic models for kimberlite pipe formation are poorly understood. Detailed geological, mineralogical, geochemical and volcanological models of individual kimberlite bodies are rare. Comparative studies of kimberlites within a kimberlite field are also rare or lacking. Note that these suggestions for future work are certainly not new ideas (see Mitchell, 1986, 1995).

A second major fundamental problem for the modern diamond explorer is knowledge of the thickness and age of lithospheric mantle roots within continental cratonic regions. The thickness aspect can be determined by seismic tomography studies (e.g., van der Lee and Frederickson, 2005). However, it is important to recognize that the present day thickness may be less than the thickness at the time of kimberlite eruption (see Geotectonic Environment).

Determining the age of the mantle lithosphere is much more problematic, as physical samples of mantle peridotite must be obtained from igneous rocks of deep seated origin (i.e., kimberlite, lamproite, ultramafic lamprophyre, alkali basalt). However, whole rock Re–Os + PGE age determination technique for mantle peridotites is quite advanced (Pearson et al., 1995, 2002; Irvine et al., 2003) and coupled with thermobarometric estimates for xenoliths, age versus depth profiles can be constructed. Alternately, less refined lithospheric age data can be construed from laser ablation Re-Os data for sulphide inclusions in forsterite (e.g., Aulbach et al., 2002; Griffin et al., 2002). Certainly, a more refined understanding of the age and formation of lithospheric mantle and its relationship to diamond formation and stability would be invaluable.

More problematic are the following questions:

1. What mantle event(s) cause diamonds to form? Are there related and identifiable events in the crust?

2. What mantle event(s) triggers the partial melting that generates kimberlite magma in the mantle? At what depth (or depths) does this occur and what are the source characteristics? Are there crustal events which also record the events that trigger kimberlite formation?

Areas of High Diamond Potential in Canada

With the largest Precambrian Shield on the Earth and diamond mines in two different Archean blocks (Slave and Superior cratons), where next should one explore in Canada? Quite a number of potential areas with high diamond potential were outlined last decade by Kjarsgaard (1998b), specifically within the Superior craton and in the enigmatic Churchill province. Since that time, quite a number of new discoveries have been made in both the Superior craton (e.g., Wemindji, Renard kimberlites) and Churchill province (e.g., Aviat, Repulse Bay, Rankin Inlet, Boothia Peninsula kimberlites). Both of these cratonic regions are quite large and are still underexplored. The lack of a comprehensive bedrock geological framework for the Rae, the south, central, and northern Hearne domains, and Queen Maude block within the Churchill province, coupled with a paucity of lithospheric mantle information makes it difficult at present to refine the search area. The northwestern (Ontario and Manitoba) and northeastern (Quebec) parts of the Superior province are also perhaps under explored, although this is due in part to thick glacial or glaciolacustrine cover. The true extent and nature of the Archean Sask craton is imperfectly known and understood, and the geometry of the Superior –Sask–Churchill terrain boundaries in the prairie provinces needs refining in order to better understand the potential for kimberlite diamond deposits in this region.

Acknowledgements

Formal manuscript reviews by Prof. D. G. Pearson and an anonymous reviewer as well as an informal review by G. Read were quite helpful. Discussions with numerous industry (BHP Billiton, De Beers, Kennecott, Shore Gold, Ashton, MPH Consulting, etc.) and various consultants and academic colleagues the past 17 years have been extremely useful. They may not agree with all the contents of this chapter! C. Jefferson (GSC) is thanked for continuing moral support. Wayne Goodfellow is thanked for editorial comments and patience. B. Hillary drafted Figure 1.

References

Allsopp, H.L., Bristow, J.W., Smith, C.B., Brown, R., Gleadow, A.J.W., Kramers, J.D., and Garvie, O.G., 1989, A summary of radiometric dating methods applicable to kimberlite and related rocks: Geological Society of Australia, Special Publication 14, p. 343–357.

Ashton, K.E., Lewry, J.F., Heaman, L.M., Hartlaub, R.P., Stauffer, M.R. ,and Tran, H.T., 2005, The Pelican thrust zone: Basal detachment between the Archean Sask Craton and Paleoproterozoic Flin Flon—Glennie Complex, western Trans-Hudson Orogen: Canadian Journal of Earth Sciences, v. 42, 685–706.

Aulbach, S., Griffin, W.L., O'Reilly, S.Y., and Kivi, K., 2002, Sulfides from the lower mantle?: Geochimica et Cosmochimica Acta, v. 66, no. 15A, p.38.

Bardet, M.G., 1965, Les gisements de diamant d'U.R.S.S.: Chron. Mines Rech. Minere, v. 65, p. 1–40.

Barnett, W.P., and Lorig, L. 2007, A model for stress controlled pipe growth: Journal of Volcanology and Geothermal Research, v. 159, p. 108–125.

Bhattacharji, S., and Smith, C.H., 1964, Flowage differentiation: Science, v. 145, p. 150–153.

Bleeker, W., Ketchum, J.W.F., and Davis, W.J., 1999, The Central Slave basement complex: Part II. Age and tectonic significance of high strain zones along the basement-cover contact: Canadian Journal of Earth Sciences, v. 36, p. 1111–1130.

Bloomer, A.G., and Nixon, P.H., 1973, The geology of the Letseng-la-terae kimberlite pipes, *in* Nixon, P.H. (ed.), Lesotho kimberlites: Maseru, Lesotho National Development Corporation, p. 20–32.

Boyer, L., 2005, Volcanology of kimberlites in the Buffalo Head Hills, Alberta: Unpublished M.Sc. thesis, Vancouver, University of British Columbia, 188 p.

Bulanova, G.P., 1995, The formation of diamond: Journal of Geochemical Exploration, v. 53, p. 1–24.

Carlson, R.W., Boyd, F.R., Shirey, S.B., Janney, P.E., Grove, T.L., Bowring, S.A., Schmitz, M.D., Dann, J.C., Bell, D.R., Gurney, J.J., Richardson,

S.H. Tredouz, M., Menzies, A.H., Pearson, D.G., Hart, J.R., Wilson, A.H., and Moser, D., 2000, Continental growth, preservation, and modification in southern Africa: GSA Today, v. 10, p. 1–7.

Carlson, S.M., Hillier, W.D., Hood, C.T., Pryde, R.P., and Skelton, D.N. 1999, The Buffalo Head Hills kimberlites: A newly discovered diamondiferous kimberlite province north-central Alberta, Canada: Red Roof Design, VIIth International Kimberlite Conference, Proceedings: The J.B. Dawson Volume, Cape Town, p. 109–116.

Chapman, J.G., and Boxer, G.L., 2004, Size distribution and analyses for estimating diamond grade and value: Lithos, v. 76, p. 369–376.

Clement, C.R., 1975, The emplacement of some diatreme-facies kimberlites: First International Kimberlite Conference, Physics and Chemistry of the Earth, v. 9, p. 51–59.

Clement, C.R., 1982, A comparative geological study of some major kimberlite pipes in the Northern Cape and Orange Free state: Unpublished Ph.D. thesis, University of Cape Town, 432 p.

Clement, C.R., and Skinner, E.M.W., 1985, A textural-genetic classification of kimberlites: Transactions of the Geological Society of South Africa, v. 88, p. 403–409.

Clement, C.R., and Reid, A.M., 1989, The origin of kimberlite pipes: An interpretation based on a synthesis of geological features displayed by Southern African occurrences: Geological Society of Australia, Special Publication 14.

Clifford, T.N., 1966, Tectono-metallogenic units and metallogenic provinces of Africa: Earth and Planetary Science Letters, v. 1, p. 421–434.

Coopersmith, H.G., 1993, *in* Sheahan, P., and Chater, A., eds., Diamonds: Exploration, sampling, and evaluation: Toronto, Prospectors and Developers Association of Canada, Short Course Proceedings, p. 173-184.

Crawford, B.B., Porritt, L., Nowicki, T., and Carlson, J.A., 2006, Key geological characteristics of the Koala kimberlite, Ekati diamond mine, Canada: Kimberlite Emplacement Workshop, Saskatoon, Saskatchewan, September 7–12, 2006, CD-ROM.

Creaser, R.A., Grütter, H.S., Carlson, J.A., and Crawford, B., 2004, Macrocrystal phlogopite Rb–Sr dates for the Ekati property kimberlites, Slave Province, Canada: Evidence for multiple intrusive episodes in the Paleocene and Eocene: Lithos, v. 76, p. 399–414.

Davis, G.L., 1977, The ages and uranium contents of zircons from kimberlites and associated rocks: Carnegie Institute of Washington. Yearbook, v. 76, p. 631–635.

Davis, G.L., 1978, Zircons from the mantle: Carnegie Institute of Washington, Yearbook v. 77, p. 805–807.

Davis, W.J., and Kjarsgaard, B.A., 1997, A Rb–Sr isochron for a kimberlite from the recently discovered Lac de Gras field, Slave Province, Northwest Canada: Journal of Geology, v. 105, p. 503–509.

Dawson, J.B., 1980, Kimberlites and their xenoliths: Berlin, Springer, 252 p.

Dawson J.B., and Hawthorne, J.B., 1973, Magmatic sedimentation and carbonatitic differentiation in kimberlite sills at Benfontein, South Africa: Journal of the Geological Society of London, v. 129, p. 61–85.

Dobbs, P.N., Duncan, D.J., Hu, S., Shee, S.R., Colgan, E.A., Brown, M.A., Smith, C.B., and Allsop, H.L., 1994, The geology of the Mengyin kimberlites, Shandong, China: Brazil, Companhia de Pesquisa de Recursos Minerais, CPRM Special Publication 1B, p. 329–345.

Drever, H.I., and Johnston, R., 1966, Picritic minor intrusions, *in* Wyllie, P.J., ed., Ultramafic and related rocks: New York, Wiley, p. 71–82.

Eggler, D.H., 1989, Kimberlites: How do they form?: Geological Society of Australia, Special Publication 14, p. 323–342.

Field, M., and Scott-Smith, B.H., 1999, Contrasting geology and near-surface emplacement of kimberlite pipes in southern Africa and Canada: Red Roof Design, VIIth International Kimberlite Conference, Proceedings: The J.B. Dawson Volume, Cape Town, p. 214–237.

Field, M., Gibson, J.G., Wilkes, T.A., Gababotse, J., and Khutjwe, P., 1997. The geology of the Orapa A/K1 kimberlite Botswana: Further insight into the emplacement of kimberlite pipes: Russian Geology Geophysics, v. 38, p. 24–39.

Fipke, C.E., Gurney, J.J., and Moore, R.O., 1995. Diamond exploration techniques emphasizing indicator mineral geochemistry and Canadian examples: Geological Survey of Canada, Bulletin 423, 86 p.

Ford, K., Keating, P., and Thomas, M.D., 2007, Overview of geophysical signatures associated with Canadian ore deposits, in Mineral deposits of Canada: A synthesis of major deposit types, district metallogeny, the evolution of geological provinces, and exploration methods, Goodfellow, W.D., ed.: Geological Association of Canada, Mineral Deposits Division, Special Publication 5, p. 939–970.

Fouch, M.J., James, D.E., Gao, S.S., Van Decar, J.C., and van der Lee, S., 2004, Mantle seismic structure beneath the Kaapvaal and Zimbabwe cratons: Transactions of the Geological Society of South Africa, v. 107, p. 33–44.

Gendzwill, D.J., and Matieshin, S.D., 1996. Seismic reflection survey of a kimberlite intrusion in the Fort à la Corne district, Saskatchewan: Geological Survey of Canada, Open File 3228, p. 241–242.

Gobba, J.M., 1989, Kimberlite exploration in Tanzania: Journal of African Earth Sciences, v. 9, p. 565–578.

Graham, I., Burgess, J.L., Bryan, D., Ravenscroft, P.J., Thomas, E., Doyle, B.J., Hopkins, R., and Armstrong, K.A.m, 1999, Exploration history and geology of the Diavik kimberlites, Lac de Gras, Northwest Territories, Canada: Red Roof Design, VIIth International Kimberlite Conference, Proceedings: The J.B. Dawson Volume, Cape Town, p. 262–279.

Griffin, W.L., Spetsius, Z.V., Pearson, N.J., and O'Reilly, S.Y., 2002, In situ Re–Os analysis of sulfide inclusions in kimberlitic forsterite: New constraints on depletion events in the Siberian lithospheric: Geochemistry, Geophysics, Geosystems—G3, v. 3, no. 11, 25 p.

Griffin, W.L., O'Reilly, S.Y., Doyle, B.J., Pearson, N.J., Coopersmith, H., Kivi, K., Malkovets, V., and Pokhilenko, N., 2004, Lithosphere mapping below the North American plate, Lithos, v. 77, p. 873–922.

Grunsky, E., and Kjarsgaard, B.A., 2007, Classification of eruptive phases of the Star kimberlite, Saskatchewan, Canada based on statistical treatment of whole-rock geochemical analyses: Applied Geochemistry, in press.

Grütter, H.S., and Apter, D.B., 1998, Kimberlite- and lamproite-borne chromite phenocrysts with "diamond-inclusion"-type chemistries [abs.]: University of Cape Town, 7th International Kimberlite Conference, Cape Town, April 13–17, 1998, p. 280–281.

Grütter, H.S., Gurney, J.J., Menzies, A.H., and Winter, F., 2004, An updated classification scheme for mantle-derived garnet, for use by diamond explorers: Lithos, v. 77, p. 841–857.

Grütter, H., Lattia, D., and Menzies, A., 2006, Cr-Saturation arrays in concentrate garnet compositions from kimberlite and their use in mantle barometry: Journal of Petrology, v. 47, p. 801–820.

Gurney, J.J., and Zweistra, P., 1995, The interpretation of the major element compositions of mantle minerals in diamond exploration: Journal of Geochemical Exploration, v. 53, p. 293–310.

Gurney, J.J, Helmstaedt, H.H., Le Roex, A.P., Nowicki, T.E., Richardson, S.H., and Westerlund, K.J., 2005, Diamonds: Crustal distribution and formation processes in time and space and an integrated deposit model: Economic Geology, 100th Anniversary Volume, p. 143–177.

Haggerty, S.E., 1982, Kimberlites in western Liberia: An overview of the geological setting in a plate tectonic framework: Journal of Geophysical research, v. 87, p. 10811–10826.

Haggerty, S.E., and Sautter, V., 1990, Ultradeep (greater than 300 km), ultramafic upper mantle xenoliths: Science v. 248, p. 993–996.

Hammer, P.T.C., Clowes, R.M., and Ramachandran, K., 2004, Seismic reflection imaging of thin kimberlite dykes and sills: Exploration and deposit characterization of the Snap Lake dyke, Canada: Lithos, v. 76, p. 359–368.

Hansom, E.K., Moore, J.M., Robey, J., Bordy, E.M., and Marsh, J.S., 2006, Re-estimation of erosion levels in Group I and II kimberlites between Lesotho, Kimberley, and Victoria West, South Africa: Kimberlite Emplacement Workshop, Saskatoon, Saskatchewan, September 7–12, 2006, CD-ROM.

Harvey, S.E., Kjarsgaard, B.A., Zonneveld, J.P., and McNeil, D., 2004, Update on kimberlite eruptive sequences, volcanic stratigraphy, and 3-D modelling of the 140/141 kimberlite complex, Fort à la Corne field, Saskatchewan: Saskatchewan Geological Survey, Summary of Investigations 2004, 2, Miscellaneous Report 2004-4.2, CD-ROM.

Harvey, S.E., Kjarsgaard, B.A., Zonneveld, J.P., Heaman, L.M., and MacNeil, D, 2006, Volcanology and sedimentology of distinct eruptive

phases at the Star kimberlite, Fort à la Corne field: Kimberlite Emplacement Workshop, Saskatoon, Saskatchewan, September 7–12, 2006, CD-ROM.

Hawthorne, J.B., 1975, Model of a kimberlite pipe: Physics and Chemistry of the Earth, v. 9, p. 1–16.

Heaman, L.M., and Kjarsgaard, B.A., 2000, Timing of eastern North American kimberlite magmatism; Continental extension of the great meteor hotspot track: Earth and Planetary Science Letters, v. 178, p. 253–268.

Heaman, L.M., Kjarsgaard, B.A., and Creaser, R., 2003, The timing of kimberlite magmatism in North America: Implications for global kimberlite genesis and diamond exploration: Lithos, v. 71, p. 153–184.

Heaman, L.M., Kjarsgaard, B.A., and Creaser, R., 2004, The temporal evolution of North American kimberlites: Lithos, v. 76, p. 377–398.

Helmstaedt, H.H., 2003, Tectonics and structural considerations in diamond exploration: Diamonds Short Course Notes, Cordilleran Round-Up, Vancouver, British Columbia, January, 29–30, 2003, 8 p.

Hoal, K.O., 2003, Samples of Proterozoic iron-enriched mantle from the premier kimberlite: Lithos, v. 71, p. 259–272.

Irvine, G.J., Pearson, D.G., Kjarsgaard, B.A., Carlson, R.W., Kopylova, M.G., and Dreibus, G., 2003, Evolution of the lithospheric mantle beneath northern Canada: A Re-Os isotope and PGE study of kimberlite-derived xenoliths from Somerset Island and a comparison to the Slave and Kaapvaal cratons: Lithos, v. 71, p. 461–488.

Jacob, D.E., 2004, Nature and origin of eclogite xenoliths from kimberlites: Lithos, v. 77, p. 295–316.

Jacob, D.E., Bizmis, M., and Salters, V.J.M., 2005, Lu-Hf and geochemical systematics of recycled ancient oceanic crust: Evidence from Roberts Victor eclogites: Contributions to Mineralogy and Petrology, v. 148, p. 707–720.

Janse, A.J.A., 1984, Kimberlites—Where and when, *in* Glover, J.E., and Harris, P.G., eds., Kimberlite occurrence and origin: Perth, University of Western Australia, Geology Department/Extension Services, Publication 8, p. 19–62.

Janse, A.J.A., 1993, The aims and economic parameters of diamond exploration, *in* Sheahan, P., and Chater, A., eds., Diamonds: Exploration, sampling, and evaluation: Toronto, Prospectors and Developers Association of Canada, Short Course Proceedings, p. 173–184.

—— 2005, The search for diamonds: Mining Journal, London, 20 p.

Jelsma, H.A., deWit, M.J., Thiart, C., Dirks, P.H.G.M., Viola, G., Basson, I.J., and Anckar, E., 2004, Preferential distribution along transcontinental corridors of kimberlites and related rocks of southern Africa: Transactions of the Geological Society of South Africa, v. 107, p. 301–324.

Kaminsky, F.V., Feldman, A.A., Varlamov, V.A., Boyko, A.N., Olofinsky, L.N., Shofman, I.L., and Vaganov, V.I., 1995, Prognostication of primary diamond deposits: Journal of Geochemical Exploration, v. 53, p. 167–182.

Katsube, T.J., and Kjarsgaard, B.A., 1996, Physical property characteristics of Canadian kimberlites: Geological Survey of Canada, Open File 3228, p. 241–242.

Kerr, D., Budkewitsch, P., Bryan, D., Knight, R., and Kjarsgaard, B.A., 2002, Surficial geology, spectral reflectance characteristics, and their influence on hyperspectral imaging as a drift prospecting technique for kimberlites in the DIAVIK Diamond Mine area, NWT: Geological Survey of Canada, Current Research, no. 2002-C4, 10 p.

Kinny, P.D., Compston, W., Bristow, J.W., and Williams, I.S., 1989, Archean mantle xenocrysts in a Permian kimberlite: Two generations of kimberlitic zircon in Jwaneng DK2, southern Botswana: Geological Society of Australia, Special Publication 14, p. 833–842.

Kinny, P.D., Griffin, B.J., Heaman, L.M., Brakhfogel, F.F., and Spetsius, Z.V., 1997, SHRIMP U–Pb ages of perovskite from Yakutian kimberlites: Russian Geology and Geophysics, v. 38, p. 97–105.

Kirkley, M.B., Kolebaba, M.R., Carlson, J.A., Gonzales, A.M., Dyck, D.R., and Dierker, C., 1998, Kimberlite emplacement processes interpreted from Lac de Gras examples [abs.]: University of Cape Town, 7th International Kimberlite Conference, Cape Town, April 13–17, 1998, 429–431.

Kirkley, M.B., Mogg, T., and McBean, D., 2003, Snap Lake field trip guide: Geological Survey of Canada, 8th International Kimberlite Conference Field Trip Guidebooks; Miscellaneous G 293, CD-ROM.

Kjarsgaard, B.A., 1996, Somerset Island kimberlite field, District of Franklin, Northwest Territories: Geological Survey of Canada, Open File 3228, p. 61–66.

——1998a, Compositional trends of spinel and mica in alkali minettes, southern Alberta, Canada: University of Cape Town, 7th International Kimberlite Conference, Cape Town, April 13–17, 1998, p. 435–437.

——1998b, Occurrence and diamond potential of kimberlites in Canada, [abs.]: Canadian Institute of Mining and Metallurgy, 100th Anniversary Meeting, Montreal, Quebec, May 4–9, p. 77.

——2003, Volcanology of kimberlite: Diamonds Short Course Notes, Cordilleran Round-Up, Vancouver, British Columbia, January, 29–30, 2003, 20 p.

——2007, On the recognition and significance of kimberlite tephra cones, tuff cones, and tuff rings: Journal Volcanology Geothermal Research, in press.

Kjarsgaard, B.A., and Levinson, A.A., 2002, Diamonds in Canada: Gems and Gemology, v. 38, no. 3, p. 208–238.

Kjarsgaard, B.A., Wilkinson, L., and Armstrong, J.A., 2002, Geology, Lac de Gras kimberlite field, central Slave province, Northwest Territories—Nunavut (NTS 76C, D, parts of E, F): Geological Survey of Canada, Open File 3238, colour map with descriptive notes, 1:250 000 scale.

Kjarsgaard, B.A., Harvey, S., Zonneveld, J.P, McNeil, D.H., Heaman, L.M., and White, D., 2004, Geology of the Star kimberlite, Saskatchewan: Saskatchewan Geological Survey, Summary of Investigations 2004, v. 2, Miscellaneous Report 2004-4.2, CD-ROM.

Kjarsgaard, B.A., Zonneveld, J.P., Grunsky, E., Heaman, L.M., McNeil, D., and Du Plessis, P., 2005, Recent advances in the geology of the Star kimberlite, Saskatchewan: Saskatchewan Geological Survey, Summary of Investigations 2005, v. 2, Miscellaneous Report 2005-4.2, CD-ROM.

Kjarsgaard, B.A., Harvey, S., Heaman, L.M., White, D., Grunsky, E., McNeil, D.H., and Zonneveld, J.P, 2006, Kimberlite eruptive sequences, volcanic stratigraphy, and emplacement of the 140/141 kimberlite, Fort à la Corne field, Saskatchewan, Canada Kimberlite Emplacement Workshop, Saskatoon, Saskatchewan, September 7–12, 2006, CD-ROM.

Kjarsgaard, B.A., Leckie, D.A. and Zonneveld, J.P., 2007. Discussion of "Geology and diamond distribution of the 140/141 kimberlite, Fort à la Corne, central Saskatchewan, Canada", by A. Berryman, B.H. Scott-Smith and B.C. Jellicoe (Lithos v. 76, p. 99 - 114). Lithos, in press.

Leckie, D.A., Kjarsgaard, B.A., Bloch, J., McIntyre, D., McNeil, D., Stasiuk, L., and Heaman L., 1997, Emplacement and reworking of Cretaceous, diamond-bearing, crater facies kimberlite of central Saskatchewan, Canada: Geological Society of America, Bulletin 109, p. 1000–1020.

Lockhart, G, Grutter, H., and Carlson, J., 2004, Temporal, geomagnetic ,and related attributes of kimberlite magmatism at Ekati, Northwest Territories, Canada: Lithos, v. 77, p. 665–682.

Lorenz, V., Zimanowski, B., Büttner, R., and Kurszlaukis, S. 1999, Formation of kimberlite diatremes by explosive interaction of kimberlite magma with groundwater: Filed and experimental aspects:. Red Roof Design, VIIth International Kimberlite Conference, Proceedings: The P.H. Nixon Volume, p. 522–528.

Luguet, A., Pearson, D.G., Jacques, A.L., Bulanova, G.P., Smith, C.B., Roffey, S., and Rayner, M.J., 2005, Archean mantle beneath the Halls Creek mobile zone, West Australia revealed by Re-Os isotopes: Geochemica Cosmochemica Acta, v. 69/10S, p. A285.

Macnae, J., 1995, Applications of geophysics for the detection and exploration of kimberlites and lamproites: Journal of Geochemical Exploration, v. 53, p. 213–244.

Marsh, J.S., 1973, Relationships between transform directions and alkaline igneous rock lineaments in Africa and South America: Earth and Planetary Science Letters, v. 18, p. 317–323.

McClenaghan, M.B., and Kjarsgaard, B.A. 2007: Indicator mineral and geochemical exploration methods for kimberlite in glaciated terrain, examples from Canada, *in* Goodfellow, W.D., ed., Mineral deposits of Canada: A synthesis of major deposit types, district metallogeny, the evolution of geological provinces, and exploration methods: Geological Association of Canada, Mineral Deposits Division, Special Publication 5, p. 983-1006.

Mitchell, R.H., 1986. Kimberlites: Mineralogy, geochemistry, and petrology: New York, Plenum Press, 442 p.

——1995, Kimberlites, orangeites, and related rocks: New York, Plenum Press, 410 p.

——1997, Kimberlites, orangeites, lamproites, melilitites, and minettes: A petrographic atlas: Thunder Bay, Ontario, Almaz Press, 243 p.

Moore, R.O., and Gurney J.J., 1985, Pyroxene solid solutions in garnets included in diamond: Nature v. 318 p. 553–555.

Moss, S., and Russell, J.K., 2006, Pyroclastic origins of the mega-graded bed at Diavik, Kimberlite Emplacement Workshop, Saskatoon, Saskatchewan, September 7–12, 2006, CD-ROM.

Moulle, M.A., 1885, Sur la géologie générale et sur le mines de diamants de L'Afrique Du Sud: Annales des Mines, Series 8, v. 7, p. 93–344.

Musacchio, G., White, D.J., Asudeh, I., and Thomson, C.J., 2004, Lithospheric structure and composition of the Archean western Superior Province from seismic refraction/wide-angle reflection and gravity modelling: Journal of Geophysical Research, B, Solid Earth and Planets, v. 109, no. 3, p. 1–28.

Naidoo, P., Stiefenhofer, J., Field, M., and Dobbe, R., 2004, Recent advances in the geology of the Koffiefontein Mine, Orange Free State, South Africa: Lithos, v. 76, p. 161–182.

Navon, O., 1999, Diamond formation in the Earth's mantle: VIIth International Kimberlite Conference, Cape Town, Proceedings: The P.H. Nixon Volume, p. 584–2604.

Nimis, P., and Taylor, W.R., 2000, Single clinopyroxene thermobarometry for garnet peridotites: Part 1: Calibration and testing of a Cr-in-cpx barometer and enstatite-in-cpx thermometer: Contributions to Mineralogy and Petrology, v. 139, p. 541–554.

Nixon, P.H., 1973, Lesotho kimberlites: Maseru, Lesotho National Development Corporation, 350 p.

Nixon, P.H., and Leahy, K., 1997, Diamond-bearing volcaniclastic kimberlites in Cretaceous marine sediments, Saskatchewan, Canada: Russian Geology and Geophysics, v. 38, p. 17–23.

Nowell, G.M., Pearson, D.G., Bell, D.R., Carlson, R.W., Smith, C.B., Kempton, P., and Noble, S.R., 2004, Hf isotope systematics of kimberlites and their megacrysts: New constraints on their source regions: Journal of Petrology, v. 45 p. 1583–1612.

Nowicki, T., Carlson, J.A., Crawford, B.B., Lockhart, G.D., Oshurst, P.A., and Dyck, D.R., 2003, Field guide to the Ekati diamond mine: Geological Survey of Canada, 8th International Kimberlite Conference Field Trip Guidebooks, Miscellaneous G 293, CD-ROM.

Nowicki, T., Porritt, L., Crawford B., and Kjarsgaard, B.A., 2007, Geochemical trends in kimberlites of the Ekati property, Northwest Territories, Canada: Insights on volcanic and resedimentation processes: Journal of Volcanology and Geothermal Research, in press.

Pearson, D.G., 1999a, The age of continental roots: Lithos, v. 48, p.171–194.

——1999b, Evolution of cratonic lithospheric mantle: An isotopic perspective: Geochemical Society, Special Publication, v. 6, p.57–78.

Pearson D.G., and Shirey, S.B., 2002, Isotopic dating of diamonds: Reviews in Economic Geology, v. 12, p. 143–172.

Pearson D.G., Boyd, F.R., Haggerty, S.E., Pasteris, J.D., Field, S.W., Nixon, P.H., and Pokhilenko, N.P., 1994, The characterization of graphite in cratonic lithospheric mantle: A petrological carbon isotope and Raman spectroscopic study: Contributions to Mineralogy and Petrology, v. 115, p. 449–466.

Pearson D.G., Carlson, R.W., Shirey, S.B., Boyd, F.R., and Nixon, P.H., 1995, The stabilization of Archean lithospheric mantle: A Re-Os study of peridotite xenoliths from the Kaapvaal craton: Earth and Planetary Science Letters, v. 134, p. 341–357.

Pearson, D.G., Irvine, G.J., Carlson, R.W., Kopylova, M.G., and Ionov, D.A., 2002, The development of lithospheric keels beneath the earliest continents: Time constraints using PGE and Re-Os isotope systematics: Geological Society of London, Special Publication, v. 199, p. 65–90.

Perron, L., 2004, Diamonds: Ottawa, Natural Resources Canada, Canadian Minerals Yearbook, 2004, 14 p.

Price, S.E., Russell, J.K., and Kopylova, M.G., 2000, Primitive magma from the Jericho Pipe, NWT, Canada: Constraints on primary kimberlite melt chemistry: Journal of Petrology, v. 41, p. 789–808

Ramsay, R.R., and Tompkins, L.A., 1994, The geology, heavy mineral concentrate mineralogy, and diamond prospectivity of the Boa Esperanca and Cana Verde pipes, Corrego D'Anta, Minas Gerais, Brazil: Brazil, Companhia de Pesquisa de Recursos Minerais, CPRM Special Publication 1B, 5th International Kimberlite Conference, Proceedings, p. 329–345.

Read, G., Grutter, H., Winter, S., Luckman, N., Gaunt, F., and Thomsen, F., 2004, Stratigraphic relations, kimberlite emplacement, and lithospheric thermal evolution, Quirico Basin, Minais Gerais State, Brazil: Lithos, v. 77, p. 803–818.

Richardson, K.A., 1996, Geophysical exploration and GIS applications: Introduction: Geological Survey of Canada, Open File 3228, p. 225–229.

Rombouts, L., 1995, Sampling and statistical evaluation of diamond deposits: Journal of Geochemical Exploration, v. 53, p. 351–367.

Ross, G.M., Parrish, R.R., Villeneuve, M.E., and Bowring, S.A., 1991, Geophysics and geochronology of the crystalline basement of the Alberta Basin, western Canada: Canadian Journal of Earth Sciences, v. 28, p. 512–522.

Ryan, C.G., Griffin, W.L., and Pearson, N.J., 1996, Garnet geotherms: A technique for derivation of P–T data from Cr-pyrope garnets: Journal of Geophysical Research, v. 101, p. 5611–5625.

Schulze, D.J., 1989, Constraints on the abundance of eclogite in the upper mantle: Journal of Geophysical Research, v. 94, p. 4205–4212.

——1994, Abundance and distribution of Low-Ca-garnet harzburgite in the sub-cratonic lithosphere of southern Africa: Brazil, Companhia de Pesquisa de Recursos Minerais, CPRM Special Publication 1A, 5th International Kimberlite Conference, p. 327–335.

——1997, The significance of eclogite and Cr-poor megacryst garnets in diamond exploration: Exploration and Mining Geology, v. 6, p. 349–366.

Scott-Smith, B.H., 2006, Canadian kimberlites: geological characteristics relevant to emplacement, Emplacement Workshop, Saskatoon, Saskatchewan, September 7–12, 2006, CD-ROM.

Shirey, S.B., Richardson, S.H., and Harris, J.W., 2004, Age, paragenesis, and composition of diamonds and evolution of the Precambrian mantle lithosphere of southern Africa: Transactions of the Geological Society of South Africa, v. 107, p. 91–106.

Simakov, S.K., 1999, Garnet—Clinopyroxene geobarometry of deep mantle eclogites and eclogite paleogeotherms: University of Cape Town, 7th International Kimberlite Conference, Cape Town, April 13–17, 1998, Proceedings, p. 783–787.

Sobolev, N.V., 1971. On mineralogical criteria of a diamond potential of kimberlites: Geologiya i Geofizika, v. 12 (3), p. 70–78 (in Russian).

——1977, Deep-seated inclusions in kimberlites and the problem of the composition of the upper mantle: Washington, American Geophysical Union, 279 p.

Sparks, R.S.J., Baker, L., Brown, R.J., Field, M., Schumacher, J., Stripp, G., and Walters, A.L., 2006, Dynamics of kimberlite volcanism: Journal of Volcanology and Geothermal Research, v. 155, p.18–48.

Stripp, G.R., Field, M., Schumacher, J.C., Sparks, R.J.S., and Cressey, G., 2006, Post emplacement serpentinization and related hydrothermal metamorphism in a kimberlite from Venetia, South Africa: Journal of Metamorphic Petrology, v. 24, p. 515–534.

Stubley, M., 2004, Spatial distribution of kimberlite in the Slave Province: A geometrical approach: Lithos, v. 77, p. 683–694.

Tappe, S., Foley, S.F., Jenner, G.A., and Kjarsgaard, B.A., 2005, Integrating ultramafic lamprophyre into the IUGS classification of igneous rocks: Rationale and implications: Journal of Petrology, v. 46, no. 9, p. 1893–1900.

van der Lee, S., and Frederiksen, A., 2005, Surface wave tomography applied to the North American upper mantle, *in* Levander, A. and Nolet, G., eds., Seismic earth: Array analysis of broadband seismograms: Washington, American Geophysical Union, p. 67–80.

Wagner, P.A., 1914, The diamond fields of South Africa: Johannesburg, Transvaal Leader, 347 p.

Walker, S., 2003, Potential field geophysics in diamond exploration:Diamonds Short Course Notes, Cordilleran Round-Up, Vancouver, British Columbia, January, 29–30, 2003, 24 p.

White, S.H., de Boorder, H., and Smith, C.B., 1995, Structural controls of kimberlite and lamproite emplacement: Journal of Geochemical Exploration, v. 53, p. 245–264.

Wilkinson, L., Kjarsgaard, B.A., LeCheminant, A.N., and Harris, J., 2001, Diabase dyke swarms in the Lac de Gras area: Significance to kimberlite exploration—initial results: Geological Survey of Canada, Current Research 2001-C8, 17 p.

Wilson, M.R., Kjarsgaard, B.A., and Taylor, B.E., 2007, Stable isotopic composition of magmatic and deuteric carbonate phases in hypabyssal kimberlite, Lac de Gras field, Northwest Territories, Canada: Chemical Geology, in press.

Wyatt, B.A., Baumgartner, M., Anckar, E., and Grütter, H., 2004, Compositional classification of kimberlitic and non-kimberlitic ilmenite: Lithos, v. 77, p. 819–840.

Zonneveld, J.-P., Kjarsgaard, B.A., Harvey, S.E., Heaman, L.M., McNeil, D.H., and Marcia, K.Y., 2004, Sedimentologic and stratigraphic constraints on emplacement of the Star Kimberlite, east-central Saskatchewan: Lithos, v. 76, p. 115–138.

Zonneveld, J.-P., Kjarsgaard, B.A., Harvey, S.E., and McNeil, D.H., 2006, Accommodation space and kimberlite edifice preservation: Implications for volcanological models of Fort à la Corne kimberlites, Kimberlite Emplacement Workshop, Saskatoon, Saskatchewan, September 7–12, 2006, CD-ROM.